



Research paper

Design, synthesis, and biological evaluation of stable $\beta^{6,3}$ -Helices: Discovery of non-hemolytic antibacterial peptides

Damodara N. Reddy ^{a,*}, Sukrit Singh ^a, Chris M.W. Ho ^a, Janki Patel ^a, Paul Schlesinger ^b, Stephen Rodgers ^c, Allan Doctor ^c, Garland R. Marshall ^{a,**}

^a Department of Biochemistry & Molecular Biophysics, Washington University School of Medicine, St. Louis, MO 63110, USA

^b Department of Cell Biology & Physiology, Washington University School of Medicine, St. Louis, MO 63110, USA

^c Department of Pediatrics, Washington University School of Medicine, St. Louis, MO 63110, USA



ARTICLE INFO

Article history:

Received 13 April 2017

Received in revised form

26 January 2018

Accepted 16 February 2018

Available online 20 February 2018

Keywords:

Gramicidin

Azaproline foldamers

Antibiotic

RBC hemolysis

Liposomes and beta-helices

ABSTRACT

Gramicidin A, a topical antibiotic made from alternating L and D amino acids, is characterized by its wide central pore; upon insertion into membranes, it forms channels that disrupts ion gradients. We present helical peptidomimetics with this characteristic wide central pore that have been designed to mimic gramicidin A channels. Mimetics were designed using molecular modeling focused on oligomers of heterochiral dipeptides of proline analogs, in particular azaproline (AzPro). Molecular Dynamics simulations in water confirmed the stability of the designed helices. A sixteen-residue Formyl-(AzPro-Pro)₈-NHCH₂CH₂OH helix was synthesized as well as a full thirty-two residue Cbz-(AzPro-Pro)₁₆-O^fBu channels. No liposomal lysis activity was observed suggesting lack of channel formation, possibly due to inappropriate hydrogen-bonding interactions in the membrane. These peptidomimetics also did not hemolyze red blood cells, unlike gramicidin A.

© 2018 Elsevier Masson SAS. All rights reserved.

1. Introduction

The design of peptide mimetics is a common strategy in medicinal chemistry due to the significant role that peptides/proteins have in molecular recognition in biology as well as their use in the improvement of ADME properties of pharmaceuticals. Organic non-peptides are used to mimic structural motifs for peptide molecular recognition as well as provide potential therapeutics for diseases. While organic scaffolds have been designed for various different types of secondary structures such as the α -helix [1,2], β -sheet [3–6] as well as less probable structures [7,8], mimetics for heterochiral secondary structures have yet to be described. Such structural motifs with alternating chirality and unique biological properties are found in nature; Gramicidin A, B and C contain heterochiral helical secondary structures with a wide central pore [9]. This helical motif was first described by Profs. G. N. Ramachandran and R. Chandrasekaran at the Second American Peptide Symposium held in Cleveland in 1968 [10] and later in 1972 [11].

Their structural analysis was based on the alternating L & D chiralities of amino acids found in gramicidins. Their postulated L,D-helix had 3.2 residues per turn and a rise of 1.55 Å per residue, and is now commonly referred to as a $\beta^{6,3}$ -helix, or LD₄-helix [11]. The carbonyl oxygens face the center of the helix and are alternatively pointed towards the amino- and carboxy-terminals generating a cation-selective channel in lipid bilayers. To quote Ramachandran & Chandrasekaran, “the LD₄-helix has the right size of cavity to bind ions like Na⁺ and K⁺, and thus appears to be the most probable helical structure for ion-transport peptides” [12–15].

Gramicidins were first isolated by Dubos in 1939 [16–18] for their bactericidal properties against gram-positive bacteria, and are still used topically as antibiotics. Due to their channel-forming properties in membranes, they show toxicity to human cells (hemolysis of red blood cells, for example), but have provided a model for antibacterial peptide research [19]. The amino acid sequence of gramicidin A (Fig. 1a) including the alternative D,L chirality was determined by Sarges and Witkop in 1964 [20–22].

Many biophysical and modeling studies on the structure of gramicidin A have been published with considerable controversy. Both a double-stranded helix and head-to-head dimer have been found depending on experimental conditions (Fig. 1b), and the topology of the preferred structure has been hotly debated. It

* Corresponding author.

** Corresponding author.

E-mail addresses: damodarareddyiisc@gmail.com (D.N. Reddy), garlandm@gmail.com (G.R. Marshall).

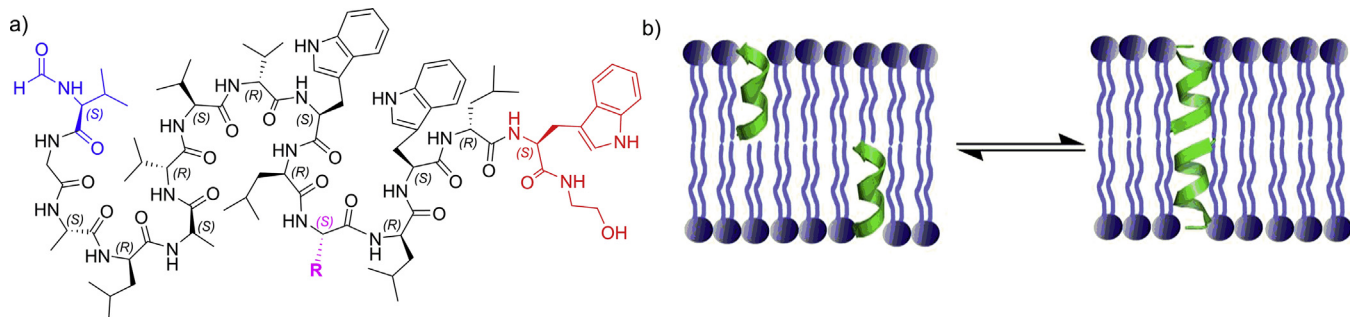


Fig. 1. a) Sequence structure of Gramicidin A monomer. R = Trp; B, R = Phe; and C, R = Tyr. b) Conformational states of gramicidin A monomers and dimers in phospholipid membranes [19].

turned out that both the head-to-head dimer and double-stranded helix conformers are present in membrane environments [19], as is the monomer. Urry et al. prepared a covalently linked head-to-head dimer that functioned as a cation-selective channel [23] supporting the conjecture of Ramachandran and Chandrasekaran of the role of $\beta^{6,3}$ -helix (LD₄-helix) in biological activity. The structure of the head-to-head dimer was later confirmed by solid-state NMR [24,25]. Another possible channel structure formed by a double-stranded helix arises from the crystal structure of gramicidin (Fig. 2) with sodium iodide [15]. The inherent conformational flexibility of gramicidins allows for multiple conformations to exist, with the preferred structure being dictated by experimental conditions (Fig. 3).

Development of a stable peptidomimetic of an *L,D*-helix ($\beta^{6,3}$ -helix) may lead a semi-rigid scaffold useful to probe channel biophysics as well as enhance the search for novel antibiotics. For example, the role of indole N-H bonding in gramicidin channel formation appears critical [30], but the mechanism remains elusive [31,32]. Are tryptophan residues essential for channel formation and antibiotic activity? Previously, it was assumed that the transitions between on and off conductance states represented Urry et al. postulated that “monomers form in the single-stranded, β -helical conformation at the interface, transiently dip into the lipid layer and remain there only if a second monomer is appropriately encountered and a lipid spanning head-to-head dimeric channel results” [33]. Based on recent solid-state NMR experiments, Jones et al. proposed that gramicidin helices undergo a conformational transition near the permeation pathway which gates the channel formation [34]. Mo et al. found a series of kinked structures with a large degree of conformational heterogeneity. The C-terminal domain was rigid with a well-defined orientation in the bilayer interfacial region. On the other hand the *N*-terminal domain,

although appearing to be conformationally rigid within the hydrophobic core of the bilayer, adopted a myriad of orientations relative to the bilayer normal [35]. Hydrophobic mismatch (defined as the difference in length between the lipid hydrophobic thickness and the peptide hydrophobic region) is thought to be responsible for altering the lipid/protein dynamics of gramicidin [36,37].

Since gramicidin has become a prototypical membrane channel, numerous potential applications of gramicidin and its analogs have emerged. Gramicidin channels can also serve as molecular force probes for studying membrane physical properties, due to their unique ability to discriminate between changes in monolayer curvature and bilayer elastic moduli, and the consequences hereafter

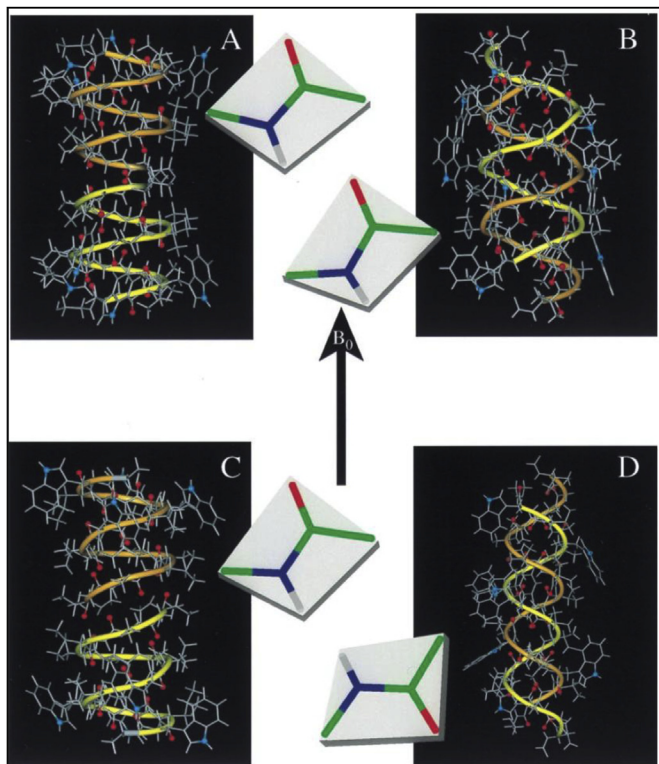


Fig. 3. Multiple conformations determined by NMR and crystallography [25]. A = Solid-state NMR-derived structure of gA from a lipid bilayer environment: single-stranded, right-handed, and 6.5 residues per turn; PDB = 1MAG [26]. B = X-ray crystallographic structure of crystals prepared from Cs⁺/MeOH solution: double-stranded, right-handed, and 7.2 residues per turn; PDB = 1AV2 [27]. C = A solution NMR structure from an SDS micellar environment: single-stranded, right-handed, and 6.3 residues per turn; PDB = 1GRM [28]. D = An X-ray crystallographic structure of crystals prepared from benzene/methanol solution: double-stranded, left-handed, and 5.6 residues per turn; PDB = 1ALZ [29].

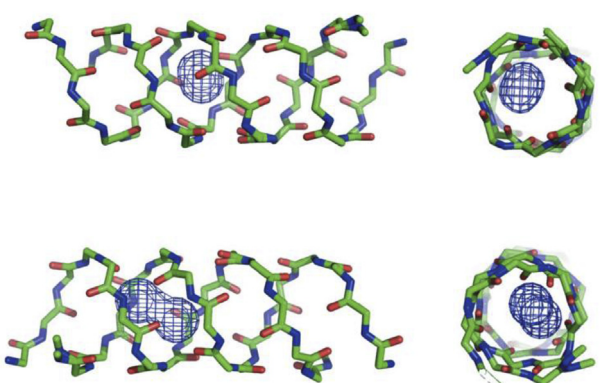


Fig. 2. Na⁺-ion positions (van der Waals surfaces) of the gA-NaI complex [15].

[38]. The mechanism of antimicrobial activity of gramicidins are still under investigation. Gramicidin A causes membrane permeabilization and induces formation of hydroxyl radicals; The latter may be the underlying mechanism of lethal activity against *Staphylococcus aureus* [39]. Solubilizing/stabilizing gramicidin by chemical modification enhances its antibacterial activity [40,41] and reduces hemolysis as well as enhances activity in selective mitochondrial uncoupling [42,43].

Simplified channels to facilitate ion movement across membranes have been investigated by Gokel [44] and others. Others have generated compounds that mimic the pore-forming properties of gramicidin A through self-assembly of smaller fragments [45,46]. To our knowledge, however, no stable peptidomimetic of the heterochiral helix formed by gramicidin A itself has been disclosed.

1.1. Approach for design

This study used molecular dynamics and molecular modeling to explore possible peptidomimetic designs for a stable oligomer of heterochiral dipeptides. The use of proline and proline analogs as the scaffold was a primary focus of this study. Oligomers of proline heterochiral dimers are excellent candidates because the dipeptides stabilize and initiate reverse turns [47,48]; a succession of turns generate helices. Multiple dimers were tested and dimers of proline and azaproline (AzPro) were chosen as azaproline was known to stabilize *cis*-amide bonds in short peptides [49]. In addition, the presence of the nitrogen replacing the α -carbon allows pyramidal inversion of the sp^3 -hybridized nitrogen costing only 5–10 kcal/mol, corresponding to interconversion between the two mirror image (*R,S*) forms [51]; this stereodynamic nitrogen allows conformational adjustment to environmental conditions. The dimer synthon is relatively easy to synthesize, and allows for the generation of repeating oligomeric motifs for probing molecular recognition. In addition, synthetic modification of the proline ring to orient different functional groups has been well documented [52], thus, it would be relatively simple to incorporate functional groups onto semi-rigid cyclic amino acids, such as proline or its homolog pipecolic acid and their analogs, for surface modulation of the peptide helices. Modular heterochiral dipeptides with different side chains appended to the cyclic ring would provide a toolkit for recognition studies. Simple modification of dipeptide units would allow for generation of multiple differing structures to probe for molecular-recognition motifs. It was found that oligomers of proline-azaproline [53,54] dimers (Pro-AzPro)_n generated stable mimetics of the heterochiral $\beta^{6,3}$ -helical secondary structure seen in gramicidins (Fig. 4c and d).

2. Computational approach

2.1. Conformational screening of candidate structures

Candidate dimers were built using Maestro (Schrodinger, Version 9.3) and to generate extended structures with total length of 30 residues. Conformer searching was done using the OpenEye OMEGA software package (version 2.5.1.4) by generating 20,000 unique conformers of the extended structure and the 10 lowest-energy conformers were output and minimized using SZYBKI (version 1.7.0) using the Poisson-Boltzmann Implicit Solvation Model. Energies for conformer stability comparisons were computed using parameters from the MMFF94 force field. The conformers were then visually evaluated, and if 7 out of the 10 conformers were similar to gramicidin A (helical with a pore and all carbonyls pointing towards the middle), the most stable conformer was used to carry out MD. This procedure is summarized in Fig. 5.

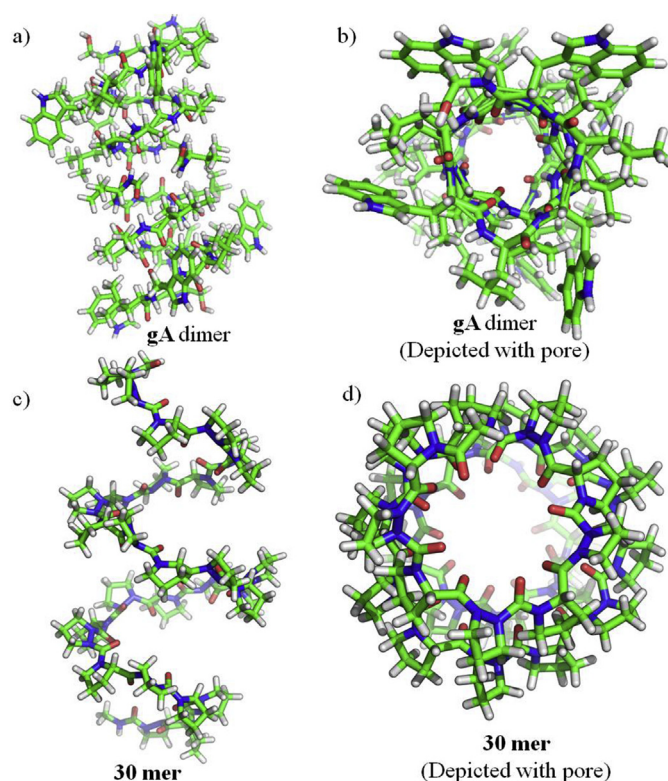


Fig. 4. a) Structures of Gramicidin A (gA) Head-to-Head Dimer Helices (PDB ID: 1NRM [50]); side and top view, b) gA Depicted with pore, c) Helical structure of Pro-AzPro 30-residue helix (30 mer) from molecular modeling; side and top view, d) 30 mer Depicted with pore.

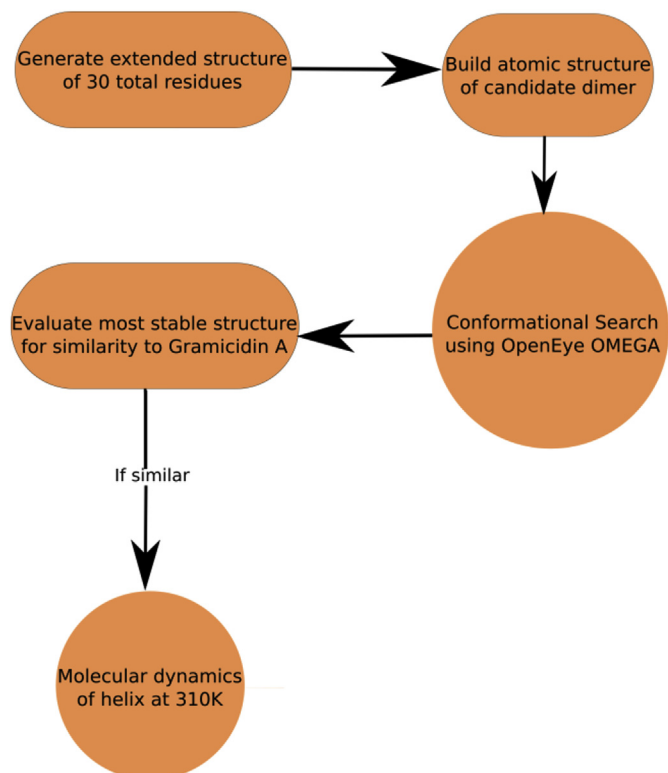


Fig. 5. Flowchart of the procedure for testing candidate dimers for helical quality.

2.2. Molecular dynamics simulation of helical structures

To further determine if the helical structures generated by the OpenEye suite were structurally stable in aqueous conditions, the most stable conformer was passed into the SYBYL molecular dynamics engine using the MMFF94 Force Field [55]. For each candidate, the most stable helical conformer was solvated in a sphere of water with a diameter of 35 Å. The structure was then minimized using a steepest descent algorithm in explicit solvent with periodic boundary conditions. MD simulation using under NVT conditions at a constant temperature of 310 K was run for 1 ns with 1 fs steps. The structure was then minimized using steepest descent once again at 310 K. Fitting to any template helices, like Gramicidin A, for RMSD and flexibility information was done via alpha-carbon atom fit, or using the nitrogen atom of AzPro analogous to the alpha carbon in the helix residues. All final energy values were obtained using the final minimized structure and normalized by dividing by the molecular weight of the helix to allow comparison. Information about the helical character and helical pore size was obtained using PyMOL [56] and the python analysis library. Backbone analysis of the helix (Fig. 6) demonstrates that both Φ and Ψ of the proline and azaproline residues are highly constrained over the course of the simulation. Both residues exist in a single state throughout, and very little variation is seen in either backbone dihedral angles. This provided initial evidence that the Pro-AzPro helical dimer would maintain a constrained helical character. However, it is important to note that this highly constrained helix was observed in simulations in water, and not necessarily indicative of the structure the helix would adopt once it was within the membrane. Furthermore, these distribution plots are derived from short simulation times.

Visualization of the simulation provides further insight into the physical basis of the torsional shape. Initial intuition would suggest that the peptide would in fact exist in equilibrium with equal tendencies to be in either the helical conformation or an unfolded non-helical shape. This is suggested by the fact that unlike naturally occurring peptide helices, there are no hydrogen bonding sites on the backbone of the Pro-AzPro helix since neither amino acid has the necessary hydrogen bond donor-acceptor combination.

However, some helical structure might occur due to the torsional forces on each proline dimer as has been discussed in the literature [53,54]. However, it was observed in the simulations that the stable helix shape was maintained due to the presence of polar solvent bridging the turns of the helix. The presence of a polar water solvent created hydrogen bonding network pathway that connected the carbonyl groups of each successive turn in the helix to one another, further stabilizing the helical shape of the peptide.

To further probe this polar-solvent bridging hypothesis, an ethanolamine solute was added to the peptide-solvent construct and simulated for an additional 50 ns. Ethanolamine was chosen due to it also having both a hydrogen bond acceptor and a hydrogen bond donor on the molecule, and had a long enough carbon chain that it would be easily visible bridging the turns of the helix. The helical structure was maintained throughout the simulation, and by the end of the simulation the ethanolamine was observed bridging the helical turns (Fig. 7). However, it is important to note that while it aided bridging the turns, it was not obstructing the pore, providing support for that the solvent-bridging hypothesis allows for stable pore formation.

Further insight into the ion binding properties of analogous peptides was sought using molecular simulation. 50 ns MD simulations were performed with SYBYL in aqueous conditions containing both Ca^{2+} and Cl^- ions. Channel structure was maintained over the course of the simulation (Fig. 8), as shown by the root-mean-square deviations (RMSD) and root-mean-square fluctuations per cyclopeptide (RMSF). 50 ns of simulation was sufficient for equilibrium sampling as indicated by the rapid entry of both water and cations into the nanotube, generally within the first nanosecond. Strong selectivity for cations is attributed to the negatively charged carbonyl oxygen atoms facing inside the channel.

3. Synthesis of gramicidin A peptidomimetics

Incorporation of an aza-amino acid residue into the peptide chain requires a combination of hydrazine and peptide chemistry by adding a protected hydrazine to an isocyanate derivative of the peptide N-terminal. Unfortunately, it is not applicable when Pro occupies the N-terminal position as in many of our cases. Andre

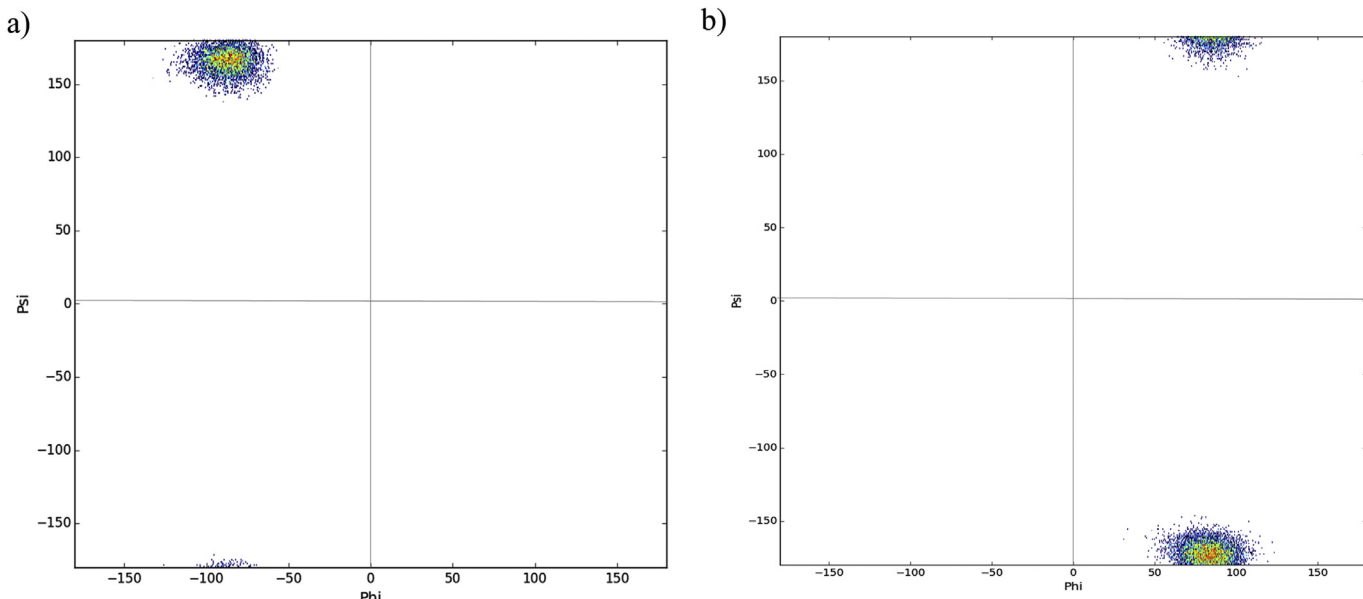


Fig. 6. Torsion distribution plots computed from molecular dynamics simulations of the AzPro-Pro oligomer. **a)** Torsion angles of all proline residues found in the oligomer. **b)** Backbone torsions of all azaproline residues found in the oligomer. The Φ angle for azaproline was computed using the α -nitrogen in place of the α -carbon.

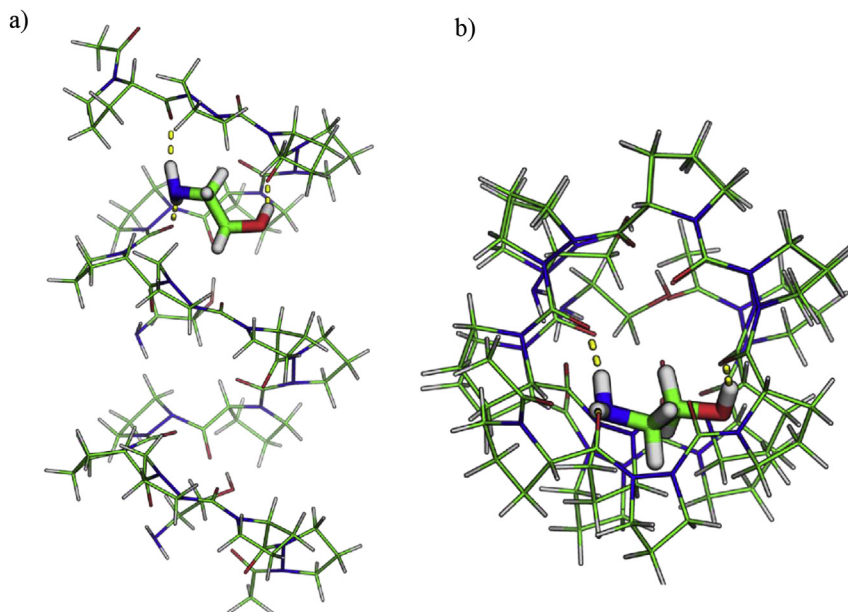


Fig. 7. a) Ac-Pro-AzPro-Ac helical structure with ethanolamine embedded demonstrating hydrogen bond bridging between turns. b) Top view demonstrating an unoccluded pore.

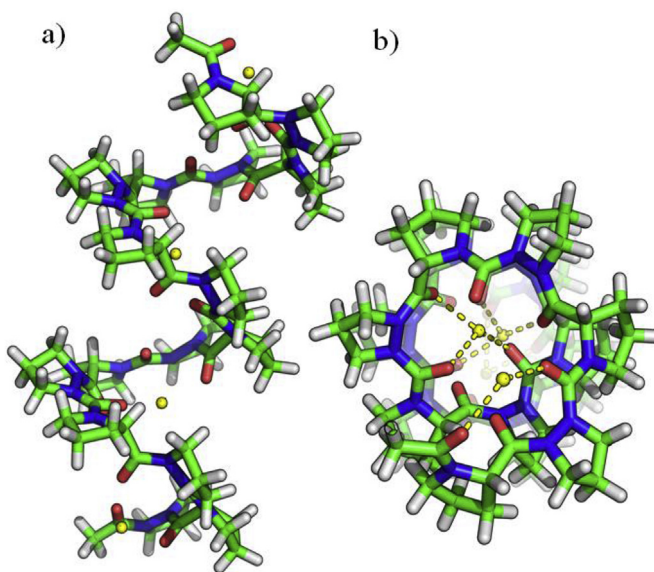


Fig. 8. a) Helical structure of Ac-(Pro-AzPro)₈-Ac (**16 mer-CaCl₂**) helix (trapped with calcium ions from molecular modeling; side view and b) top view.

et al. [57] used triphosgene as the carbonylating reagent of a protected hydrazide and it is a mild, easy to handle, and an efficient carbonylating agent for the azapeptide synthesis. Although this method works well, in general, but the activated species can only be prepared *in situ* (under N₂ at –10 °C), and formation of considerable amounts of side products, such as diazatides, were observed. More recently, synthetic routes to azapeptides have been investigated by Zhang et al. [50,54] using a liquid-phase approach. Utilizing this synthetic strategy, we have synthesized a wide variety of Pro-AzPro-containing gramicidin A analogs including a full length 32-residue peptide listed in Table 1.

Initially, we synthesized the azaproline peptide (Scheme 1) starting from Boc-hydrazine (25) which was acylated by carbobenzyloxylchloride (Cbz-Cl) to afford Boc-NH-NH-Cbz (26) with an

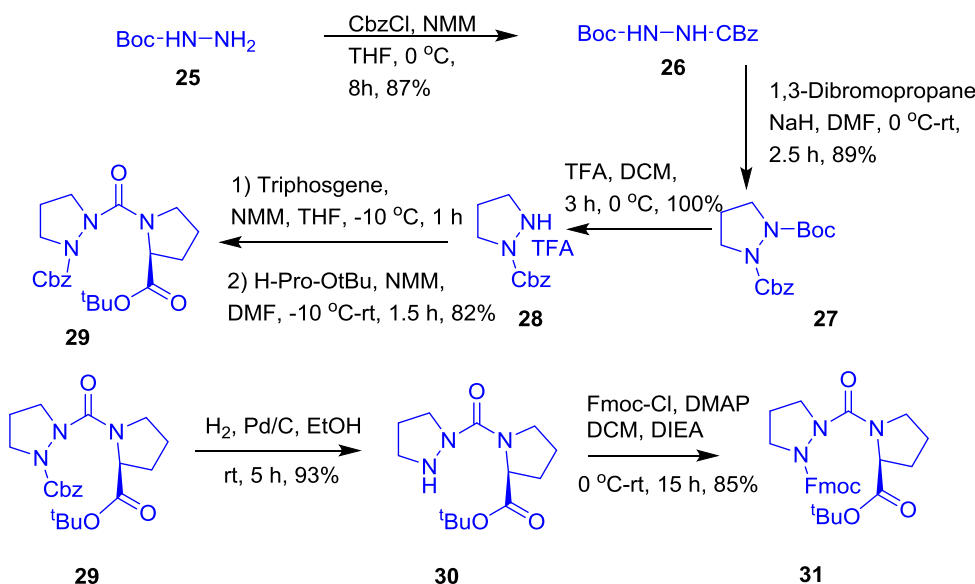
excellent yield. Then the compound **26** was reacted with NaH in DMF and subsequent treatment by 1,3-dibromopropane furnished Boc-AzPro-OBzl (**27**). Boc group was deprotected by using 20% trifluoroacetic acid in dichloromethane to give Cbz-*N,N'*-propylhydrazine (**28**) quantitatively, which was activated with triphosgene at –20 °C in tetrahydrofuran (THF), and then treated with H-Pro-O^tBu to give the Cbz-AzPro-Pro-O^tBu dipeptide (**29**) in good yield. Removal of Cbz by hydrogenation gave H-AzPro-Pro-O^tBu (**30**), which was acylated with Fmoc-Cl in presence of a catalytic amount of DMAP to afford Fmoc-AzPro-Pro-O^tBu (**31**); then O^tBu ester group was deprotected using 30% trifluoroacetic acid in dichloromethane furnished Fmoc-AzPro-Pro-OH (**32**) acid quantitatively and then we initiated solid phase peptide synthesis for making AzPro-Pro-oligomers. Fmoc-AzPro-Pro-OH (**32**) was loaded into 2-chlorotriptyl resin in DCM by using DIEA (see supplementary material S1.4, page S6). Then N-terminal Fmoc group was deprotected using 20% piperidine in DMF, but α-dehydrogenated azaproline was observed instead, which was further conformed by treating compound **31** with 20% piperidine in DMF, offered exclusively eliminated product (see supplementary material S1.4, page S6). The free azaproline peptides undergo α-elimination to give pyrazolidine derivatives even without any base, this spontaneous elimination was examined in all unprotected azaproline peptides.

Finally, we chose the other option, solution phase synthesis, dipeptide **29** was made into two parts; first, the O^tBu ester group was deprotected with trifluoroacetic acid to obtain Cbz-AzPro-Pro-OH (**34**) quantitatively. Removal of Cbz by hydrogenation of a second sample gave H-AzPro-Pro-O^tBu (**30**). Cbz-(AzPro-Pro)₂-O^tBu (**35**) tetrapeptide was prepared by using HATU peptide coupling protocol (Scheme 2). Using a similar synthetic strategy, Cbz-(AzPro-Pro)4-O^tBu octamer (**18**), Cbz-(AzPro-Pro)₈-O^tBu hexadecamer (**10**), and 32-mer Cbz-(AzPro-Pro)₁₆-O^tBu (**11**) were prepared.

Peptide Cbz-(AzPro-Pro)₈-O^tBu hexadecamer (**10**), the Cbz protecting group was deprotected by catalytic hydrogenation with masking of the deprotected azaproline with HCl. Further formylation used formic acid and acetic anhydride. Then N-terminal proline-O^tBu was deprotected using 4 N HCl in 1,4-dioxane at 50 °C; in addition to the cleavage of the O^tBu ester, the formyl group also cleaved and dimer-shortened fragments were generated as shown

Table 1List of synthesized AzPro-Pro peptide analogs, gramicidin A (**gA**) and their molecular weights.

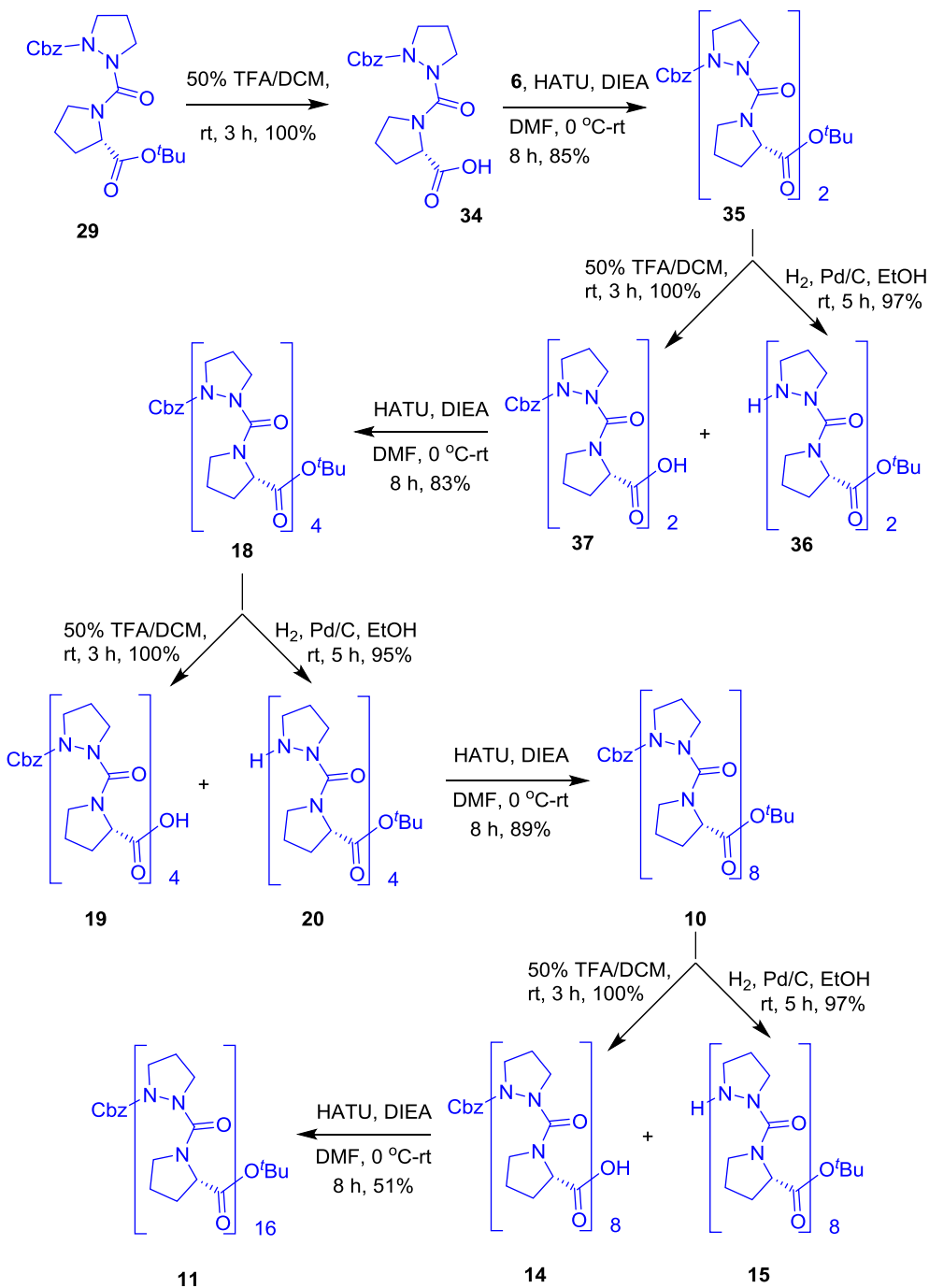
S. No.	Sequence	Compound code	Reaction code	Molecular weight
1	Cbz-(AzPro-Pro) ₈ -NHCH ₂ CH ₂ OH	1	NDR-487	1756.99
2	Ac-(AzPro-Pro) ₈ -NHCH ₂ CH ₂ OH	2	NDR-488	1664.90
3	Formyl-(AzPro-Pro) ₈ -NHCH ₂ CH ₂ OH	3	NDR-363	1650.87
4	H-(AzPro-Pro) ₈ -NHCH ₂ CH ₂ OH	4	NDR-16MER	1622.86
5	Formyl-(AzPro-Pro) ₇ -NHCH ₂ CH ₂ OH	5	NDR-14MER	1455.65
6	Formyl-(AzPro-Pro) ₆ -NHCH ₂ CH ₂ OH	6	NDR-12MER	1260.43
7	Formyl-(AzPro-Pro) ₅ -NHCH ₂ CH ₂ OH	7	NDR-10MER	1065.21
8	Cbz-(AzPro-Pro) ₈ -O ^t Bu	8	NDR-350	1770.03
9	H-(Pro-AzPro) ₈ -H	9	NDR-489	1533.77
10	Boc-(Pro-AzPro) ₈ -Cbz	10	NDR-409	1770.03
11	Cbz-(AzPro-Pro) ₁₆ -O ^t Bu	11	NDR-353	3331.81
12	Boc-(Pro-AzPro) ₈ -COOMe	12	NDR-477	1693.93
13	Cbz-(AzPro-Pro) ₈ -(N-Methyl AzPro)	13	NDR-354	1782.05
14	Cbz-(AzPro-Pro) ₈ -OH	14	NDR-451	1713.93
15	HCl.H-(AzPro-Pro) ₈ -O ^t Bu	15	NDR-452	1672.36
16	HCl. H-(Pro-AzPro) ₈ -Cbz	16	NDR-478	1706.37
17	Boc-(Pro-AzPro) ₈ -H.HCl	17	NDR-479	1770.03
18	Cbz-(AzPro-Pro) ₄ -O ^t Bu	18	NDR-347	989.14
19	Cbz-(AzPro-Pro) ₄ -OH	19	NDR-348	933.04
20	H-(AzPro-Pro) ₄ -O ^t Bu	20	NDR-349	855.01
21	Boc-(Pro-AzPro) ₄ -Cbz	21	NDR-403	989.14
22	Boc-(Pro-AzPro) ₄ -H	22	NDR-375	855.01
23	HCl.H-(Pro-AzPro) ₄ -Cbz	23	NDR-476	925.49
24	Formyl-L-Val-Gly-L-Ala-D-Leu-L-Ala-D-Val-L-Trp-D-Leu-L-Trp-D-Leu-L-Trp-D-Leu-L-Trp-NHCH ₂ CH ₂ OH	24	gA	1882.29

**Scheme 1.** Synthesis of protected Fmoc-AzPro-Pro-O^tBu dipeptide.

in **Scheme 3**. We further formylated the mixture of dimer-shortened peptides furnished mixture of compounds **39**, **40**, **41** and **42** (see the detailed LCMS data in supporting supplementary material S8, page S32), followed by coupling with ethanolamine in the presence of EDCL to generate dimer-fragmented gramicidin A analogs (see the detailed LCMS data supplementary material S8, page S33). All of them were well separable by HPLC and isolated major fractions are decamer, dodecamer, tetradecamer and hexadecamer (**7**, **6**, **5** and **3** respectively). No dimer shortened

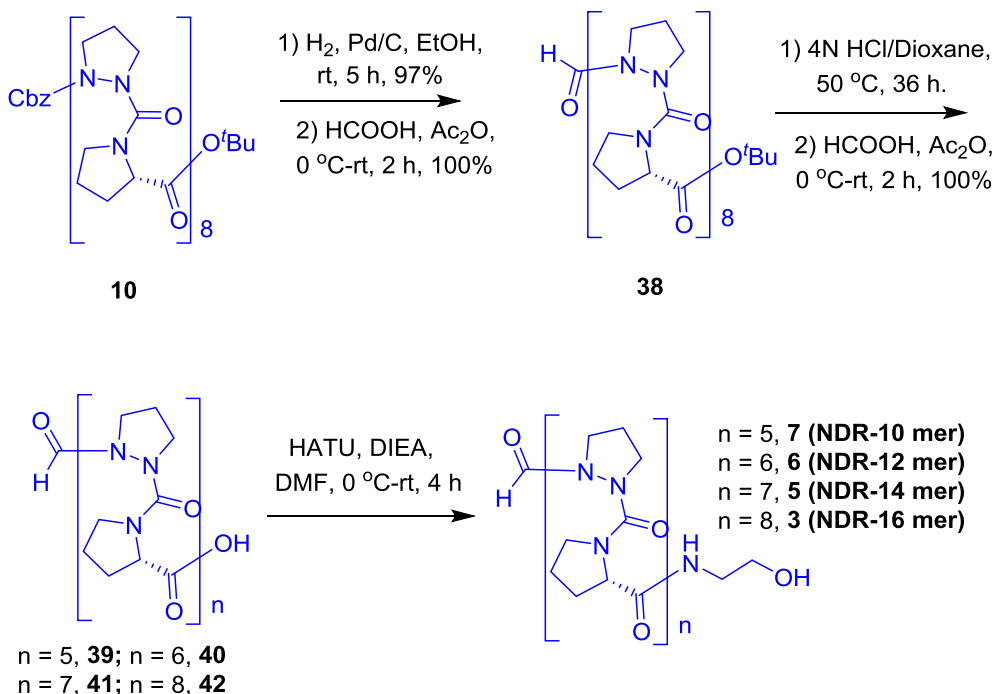
fragments were generated using 4 N HCl in 1,4-dioxane at 22°C, but the reaction was rather slow. Selectively O^tBu ester was cleaved quantitatively under 50% TFA/DCM conditions; insertion of ethanolamine produces a formylated **gA** analog as a single compound as shown in **Scheme 4**.

These formyl protected **gA** peptidomimetics of different lengths (10, 12, 14 & 16) were unstable, undergoing auto deformylation with time and labile with temperature also. The peptides are stable upon replacing formyl with acetyl or carboxybenzyl at the *N*-terminus of

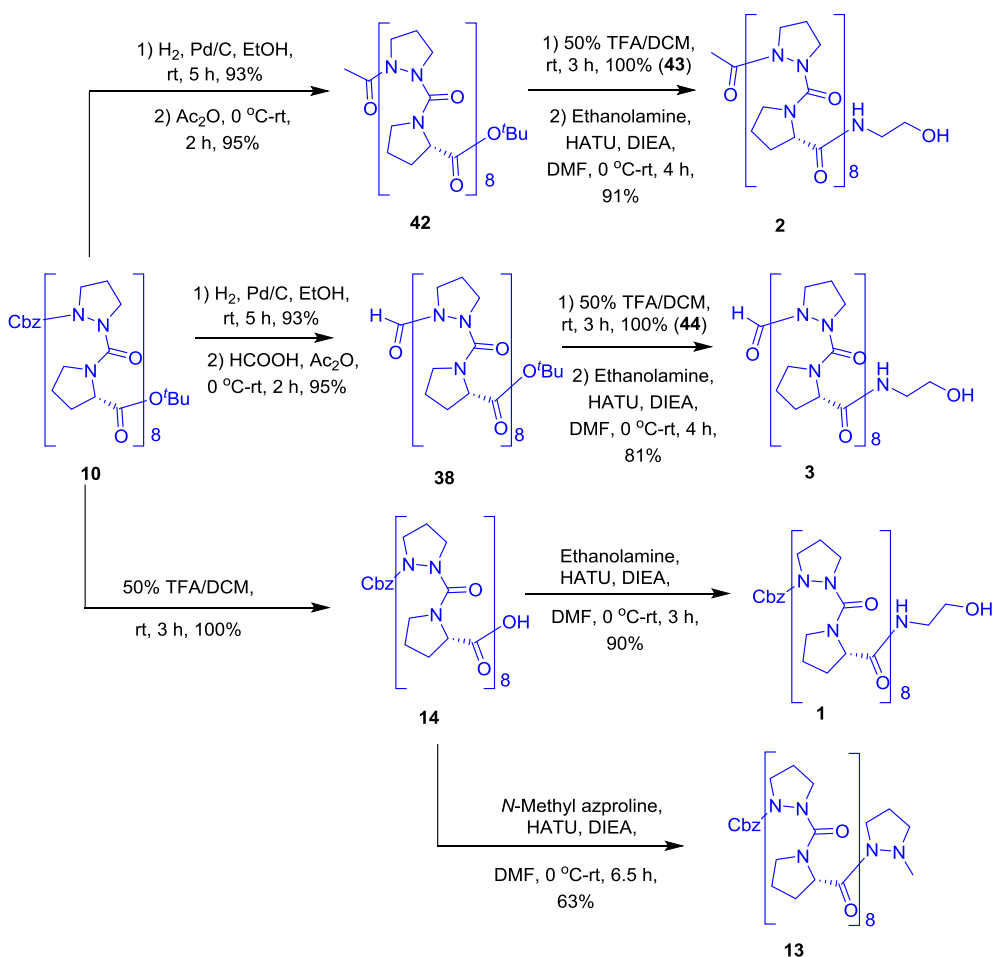
**Scheme 2.** Solution phase synthesis of Cbz-(AzPro-Pro)_n-O'Bu oligomeric peptides.

AzPro residues. Peptide Cbz-(AzPro-Pro)₈-O'Bu hexadecamer (**17**) had its Cbz protecting group cleaved under catalytic hydrogenation and further acetylated using acetic anhydride to furnish the acetylated hexadecamer O'Bu ester (**42**). C-terminal proline-O'Bu was deprotected quantitatively with 50% TFA/DCM followed by coupling with ethanolamine using the standard HATU method gave **gA** analogous peptide **2** in high yield (Scheme 4). Deprotection of C-terminal proline-O'Bu ester of peptide **10** generated the hexadecamer free acid **14**, followed by insertion of ethanolamine produce the carboxybenzylated **gA** peptide analog **1** and coupling with *N*-methyl AzPro generated peptide **13** as represented in Scheme 4.

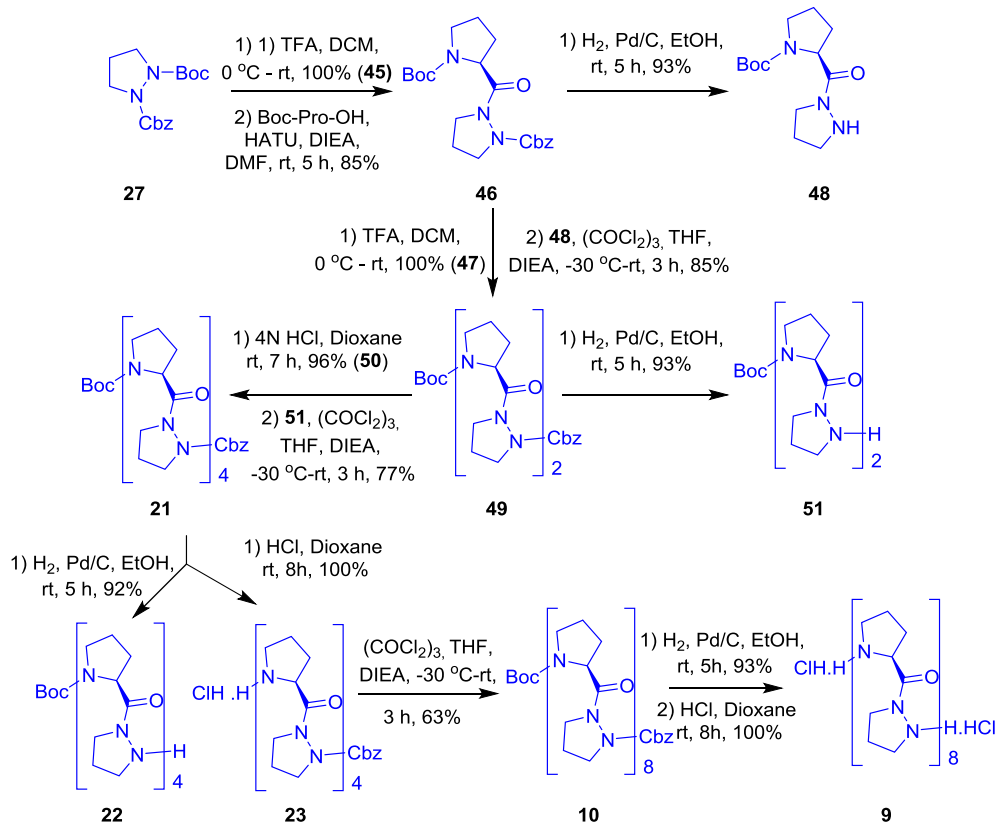
The other sequence where proline is present at the *N*-terminus and azaproline at the C-terminus of $\beta^{6,3}$ -helical peptidomimetics is represented in Scheme 5. Due to resonance, azaproline amine in H-AzPro-Cbz (**45**) is a poorer nucleophile than proline. We attempted many methods (see supplementary material S1.1, page No. S3) to couple **45** with Boc-Pro-OH. Finally, Dipeptide **46** was obtained in excellent yield by HATU coupling of Boc-Pro-OH and Cbz-AzPro-H (**45**) which was obtained by selective Boc deprotection using 50% TFA/DCM. Then dipeptide **46** was divided into two parts, the Boc group was deprotected with TFA to obtain TFA. H-Pro-AzPro-Cbz (**48**) quantitatively, removal of Cbz by hydrogenation from the other part gave Boc-Pro-AzPro-H. We were unsuccessful in



Scheme 3. Generation of a set of formyl-(AzPro-Pro)-oligomers by limited acid hydrolysis in 4 N HCl/dioxane followed by addition of C-terminal ethanolamine to form gA peptidomimetics of different lengths (10, 12, 14 & 16).



Scheme 4. Synthesis of gramicidin A analogous peptides.

**Scheme 5.** Synthesis of Boc-(Pro-Aza)₈-Cbz gramicidin analogous peptide.

connecting two fragments with a urea bond using 1,1'-carbonylidimidazole. After several attempts (see supplementary material S1.2, page No. S4), we succeeded in making Boc-(Pro-AzPro)₂-Cbz tetrapeptide (**49**) using triphosgene and N-methylmorpholine (NMM) in THF (Scheme 5). Using a similar synthetic strategy, Boc-(Pro-AzPro)₄-Cbz octamer (**21**), hexadecamer **10** (Boc-(Pro-AzPro)₈-Cbz) and unprotected hexadecamer **9** were generated.

3.1. Circular dichroism studies

The conformational states of **gA** and Pro-AzPro peptides were studied by circular dichroism spectroscopic using a JASCO CD spectrometer. All samples were prepared in PBS buffer and methanol at a concentration of 100 μM and a quartz cuvette with a 0.1 mm path length was used for the wavelength scans. The CD spectra were recorded from 190 to 260 nm in MeOH and 200–260 nm range in PBS buffer at 25 °C, with a spectrometer bandwidth of 1 nm and average of five scans.

The CD spectrum of any molecule under given conditions provides the sum of the spectra of all the individual conformers present in solution weighted by their relative abundance. The CD spectrum of purified gramicidin A (**gA**) in methanol displays two strong negative absorption bands at 210 nm and 228 nm as shown in Fig. 9a. These absorption bands can be attributed to the various forms of intertwined double helical species present in this solvent [58,59] and a distinctive positive band at 223 nm thought to be monomeric state [60–62]. Fig. 9a represents the CD spectra of all 16-mer **gA** analogous peptides; (**1–3**, **8**, and **10**) show positive absorption band attributed at 223 (θ_{max} at 223 nm) that are similar to that of **gA** monomeric n→π* transition (θ_{max} at 223 nm) that is indicative of structural persistence. Indeed the full length 32-mer (**11**) shows a similar pattern. CD spectra of the series of dimer-

shortened fragmented peptide analogs are plotted in Fig. 9b and shows θ_{max} at 221 nm for hexadecamer **4**, 218 nm for tetradecamer **5**, 216 nm for dodecamer and 214 nm for decamer which clearly supports structural deviation from beta helix in 16mer (**4**) to reverse turn in the 10mer (**7**). Fig. 9c represents the comparison of CD spectra of a series of 32mer to dipeptides Cbz-(AzPro-Pro)_n-O^tBu (n = 16(**11**), 8(**8**), 4(**18**), 2(**29**), 1(**35**)), reveals that 32mer and 16mer adopt a β^{6,3}-helical structure in methanol, whereas the octamer is blue shifted to 214 nm while the tetrapeptide and dipeptide CD spectra (θ_{max} at 211 nm) support a reverse-turn conformation. Similar CD pattern (Fig. 9d) were observed in the Boc-(Pro-AzPro)_n-Cbz (n = 8(**10**), 4(**21**), 2(**49**), and 1(**46**)) series as well.

Fig. 10a represents the CD spectrum of **gA** (dissolved in 1:1 of PBS buffer in ethanol) and peptide analogous (**1–3**, **8**, and **10**) including 32-mer (**11**) in PBS buffer shows distinctive positive absorption band attributed at 223 (θ_{max} at 223 nm) that are similar to that of **gA** monomeric n→π* transition (θ_{max} at 223 nm) which is indicative of structural persistence. CD spectra of the series of dimer-shortened fragmented peptide analogs in PBS buffer are plotted in Fig. 10b shows θ_{max} at 221 nm for hexadecamer (**3**), 218 nm for tetradecamer (**5**), 216 nm for dodecamer (**6**) and 214 nm for decamer (**7**) which clearly supports structural deviation from beta helix in 16mer (**4**) to reverse turn in the 10-mer (**7**).

3.2. Hemolysis of erythrocytes (red blood cells, RBCs)

One limitation restricting the use of gramicidin A as an antibiotic is its toxicity with human membranes as exemplified by lysis of erythrocytes. The peptidomimetic analogs were tested for RBC hemolysis by direct comparison with gramicidin A (Fig. 11). As shown, the peptidomimetic analogs demonstrated little, if any,

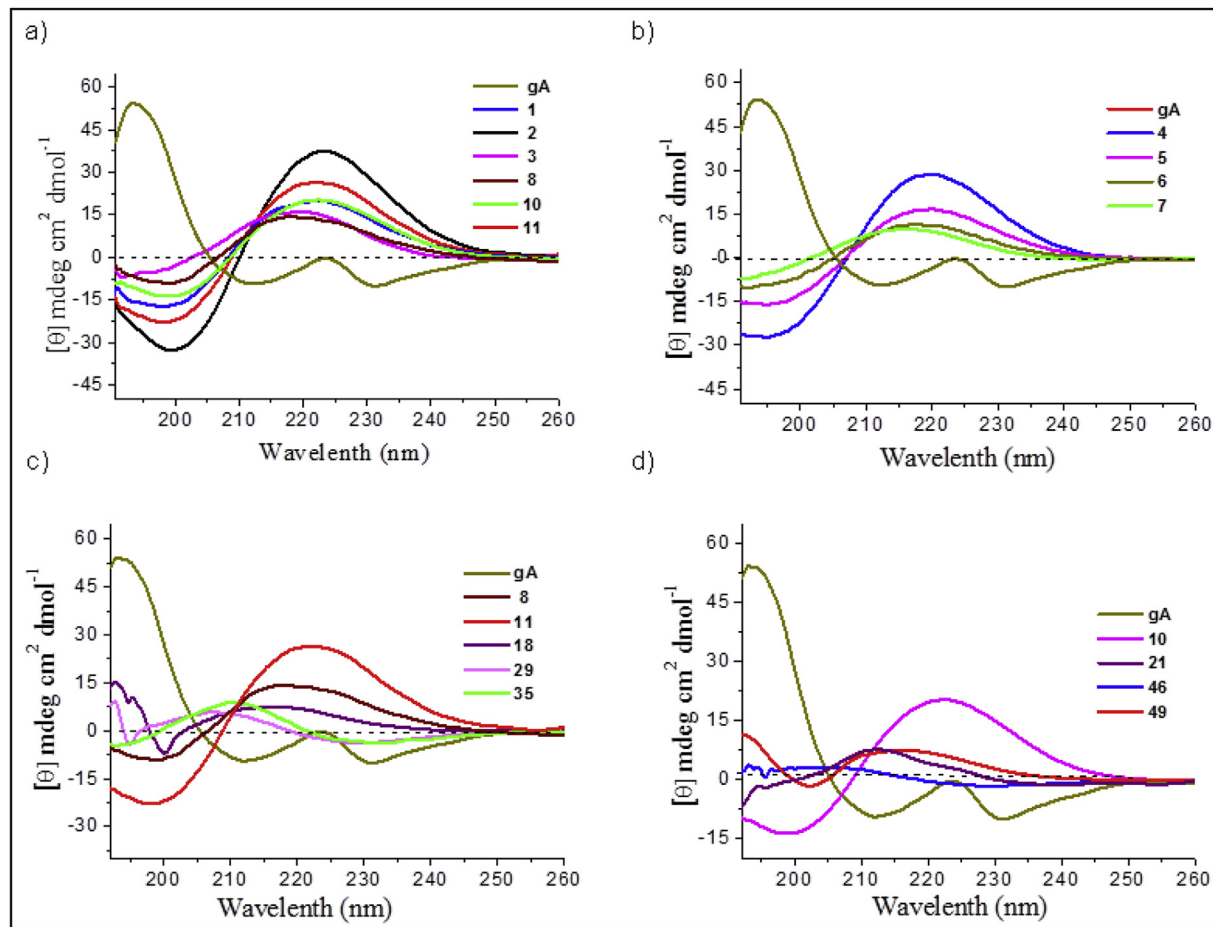


Fig. 9. CD spectrum comparision of **gA** and its analogous peptides in methanol (100 μM) at 25 $^{\circ}\text{C}$. a) gramicidin A (**gA**) and its analogous peptides (**1–3, 8, and 10**) hexadecamers and **11** is the full-length 32mer. b) **gA**, its analog **3** and dimer shortened peptides (**39–41**). c) **gA** and Cbz-(AzPro-Pro) $_n$ -O'Bu ($n = 16$ (**11**), 8(**8**), 4(**18**), 2(**29**), 1(**35**)) analogous peptides. d) **gA** and Boc-(AzPro-Pro) $_n$ -Cbz ($n = 8$ (**10**), 4(**21**), 2(**49**), 1(**46**)) analogous peptides.

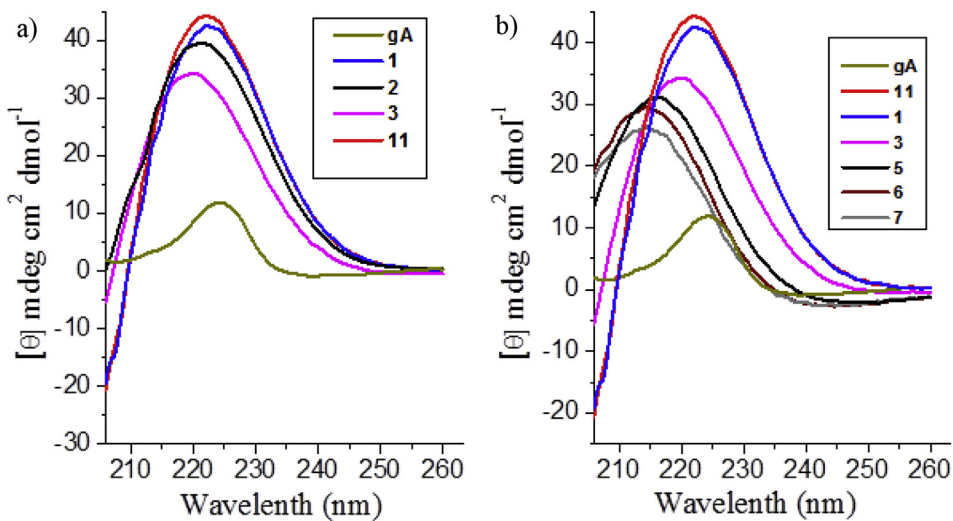


Fig. 10. Comparison of far-UV CD spectrum of gramicidin A (**gA**) and its analogous peptides in PBS buffer (100 μM) at 25 $^{\circ}\text{C}$. a) gramicidin A (**gA**) and its analogous hexadecamers (**1–3**) and **11** is the full-length 32mer. b) **gA**, **2**, **3**, **11** and dimer shortened peptides (**5–7**).

dose-dependent hemolysis as compared with authentic gramicidin A (**gA**) with a reported $\text{HC}_{50} = 5 \mu\text{M}$ [63]. Mao et al. have demonstrated that a gramicidin A analog having lactam-bridged between

the side chains of the fourth lysine and tenth glutamic acid residues stabilize the $\beta^{6,3}$ -helical conformation while significantly eliminating most antibacterial activity as well as RBC hemolysis [41].

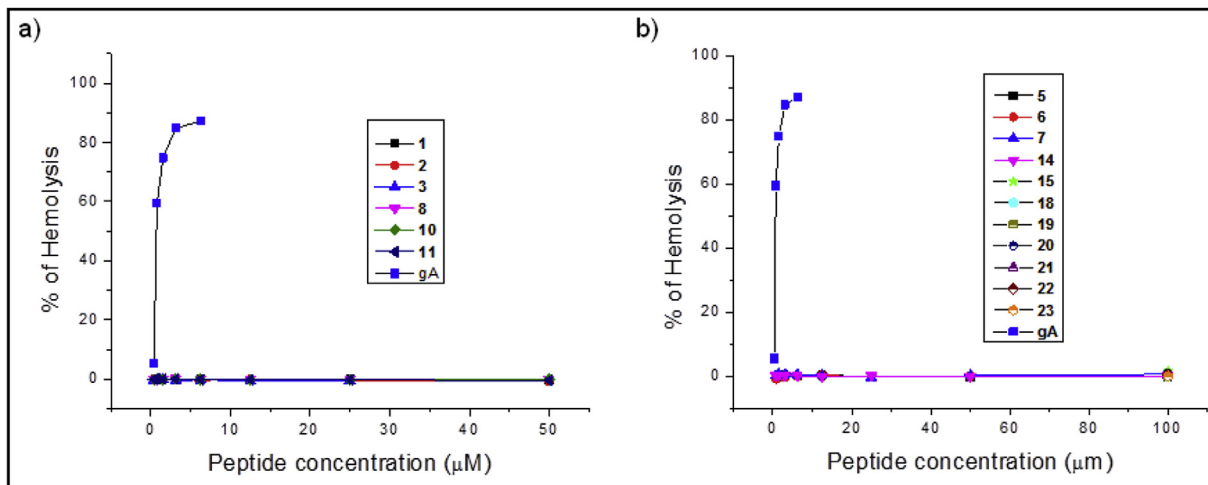


Fig. 11. RBC hemolysis comparison: a) gA and its hexadecameric analogous peptides. b) gA and shorter peptide analogs.

This suggests that the stabilized helix may not be the bioactive conformation, rationalizing our results.

3.3. Binding assays of peptides on immobilized liposomes by surface plasmon resonance (SPR) spectroscopy

We used surface plasmon resonance (Reichert) to (i) obtain more information on the modes of binding of peptides with liposomes, and ii) to determine the binding kinetics and affinity of liposomes with analogous peptides. SPR binding experiments were conducted using a Reichert SR7100DC SPR instrument. HEPES buffer (10 mM HEPES, 2-[4-(2-hydroxyethyl)piperazin-1-yl]ethanesulfonic acid; 100 mM KCl at pH 7.4) was used as a running buffer for the SPR assay. Carboxyl groups on a dextran-coated chip surface activated with N-hydroxysuccinimide, followed by covalent bonding of the ligands to the chip surface via amide linkages with 5-hydroxy sphingosine lipid and excess activated carboxyls were blocked with ethanalamine. Reference surface prepared in the same manner, except that all carboxyls are blocked and no ligand is added. A liposome solution (5 mg mL⁻¹) in PBS at a flow rate of 25 μL min⁻¹ was used to form anti-LPS-liposome complexes on the chip surface and coverage of the chip surface by the liposome complexes was assessed by a protein standard (BSA). During analysis, peptides in PBS solutions were passed over the immobilized liposome complexes at a rate of 25 μL min⁻¹ and the final concentration of bound ligand, expressed in response units (RU), which is calculated by subtracting the reference RU from the ligand RU. The chip surface is regenerated by removal of analyte with a 20 mM CHAP solution followed by immobilizing with liposomes. The changes of SPR signal as a function of time deliberates the accumulation of adsorbed peptide on the immobilized liposome. The maximum RU with each analyte demonstrates the level of interaction, and reflects comparative binding affinity.

All hexadecamer peptides (**1**, **2**, **8** and **10**) were introduced to the POPC lipid systems at 100 μM concentration and showed some binding response. We did not succeed with gramicidin A, because it was solubilised in DMSO and precipitated out of solution upon diluting with assay buffer. The sensorgrams of each peptide (**1**, **2**, **8** and **10**) binding at difference concentrations from 1000, 500, 250, 100, 50, 25 and 10 μM to the POPC lipid system are shown in Fig. 12, which indicate that the initial binding of each peptide to the model membrane is rapid and the response was also proportional to peptide concentration. At above 100 μM concentration, the peptides dissociated very little after the introduction of peptides

(Fig. 12), suggesting that these peptides have just associated with lipid vesicles instead of rupturing the liposomes. The maximum response of each concentration plotted with peptide concentration to determine the equilibrium dissociation constant (K_D) and R_{max} for analogous peptides **1**, **2**, **8** and **10** as shown in Fig. 12.

Peptide **1** and **10** showed higher affinity binding with a K_D of 3.7×10^{-4} M, 4.4×10^{-4} M respectively. A weaker affinity was observed for peptide **2** (6.1×10^{-4}) and **8** (2.58×10^{-3}). We therefore conclude that these peptides have a low affinity for POPC liposomes. A weaker affinity interaction could be due to the peptide not making a channels within the liposome membrane.

3.4. Liposomal assay of channel formation

Liposome preparation and efflux was followed according to Saito et al. [64] 1-Palmitoyl-2-oleoyl-sn-glycero-3-phosphocholine (POPC) and 1,2-dioleoyl-sn-glycero-3-phosphocholine (DOPC) (Avanti Polar Lipids) composition of liposomes was used for all experiments. 5 mg of lipid was dissolved in chloroform (1 mL), and evaporated chloroform under N₂ gas, and residual chloroform was removed using freeze dryer for 2 h, dissolved in 0.5 mL diethyl ether and hydrated in 0.5 mL HEPES buffer (10 mM HEPES, 100 mM KCl, pH 7.4, containing carboxyfluorescein (CF) - 50 nM). The azeotropic mixture was sonicated for 30 s in a bath sonicator (1600 W) for five cycles and removed residual ether under reduced pressure. Liposomes were downsized using 200 nm polycarbonate filters (Nucleopore, Pleasanton, California) by passes 11 times in a handheld, small-scale extruder (Avestin Europe GmbH, Mannheim, Germany) and separated from unincorporated fluorescein compounds by Sephadryl S-300 (Sigma) chromatography. Liposome size was determined by dynamic light scattering method using an N4MD submicron particle analyser (Coulter, Hialeah, Florida) and CF vesicles were used at 2.2×10^{10} vesicles per mL.

Using a monodisperse preparation of liposomes, we undertook the quantitative study of gA-peptidomimetic pore formation. In these liposomes the CF at quenching concentrations; dequenching can be resulted by release of CF from liposome vesicles of this size upon rupturing. The kinetics of pore activation could be monitored experimentally by the dequenching rate. Gramicidin A and a series of (AzPro-Pro)_n peptide analogs, were tested to determine the impact of channel length on release of CF. In all the peptides and gA were tested at 20 μM concentration and peptide solution was mixed with vesicle for 3 min of equilibration. Fig. 13a represents the POPC liposome leakage comparison of gramicidin A with

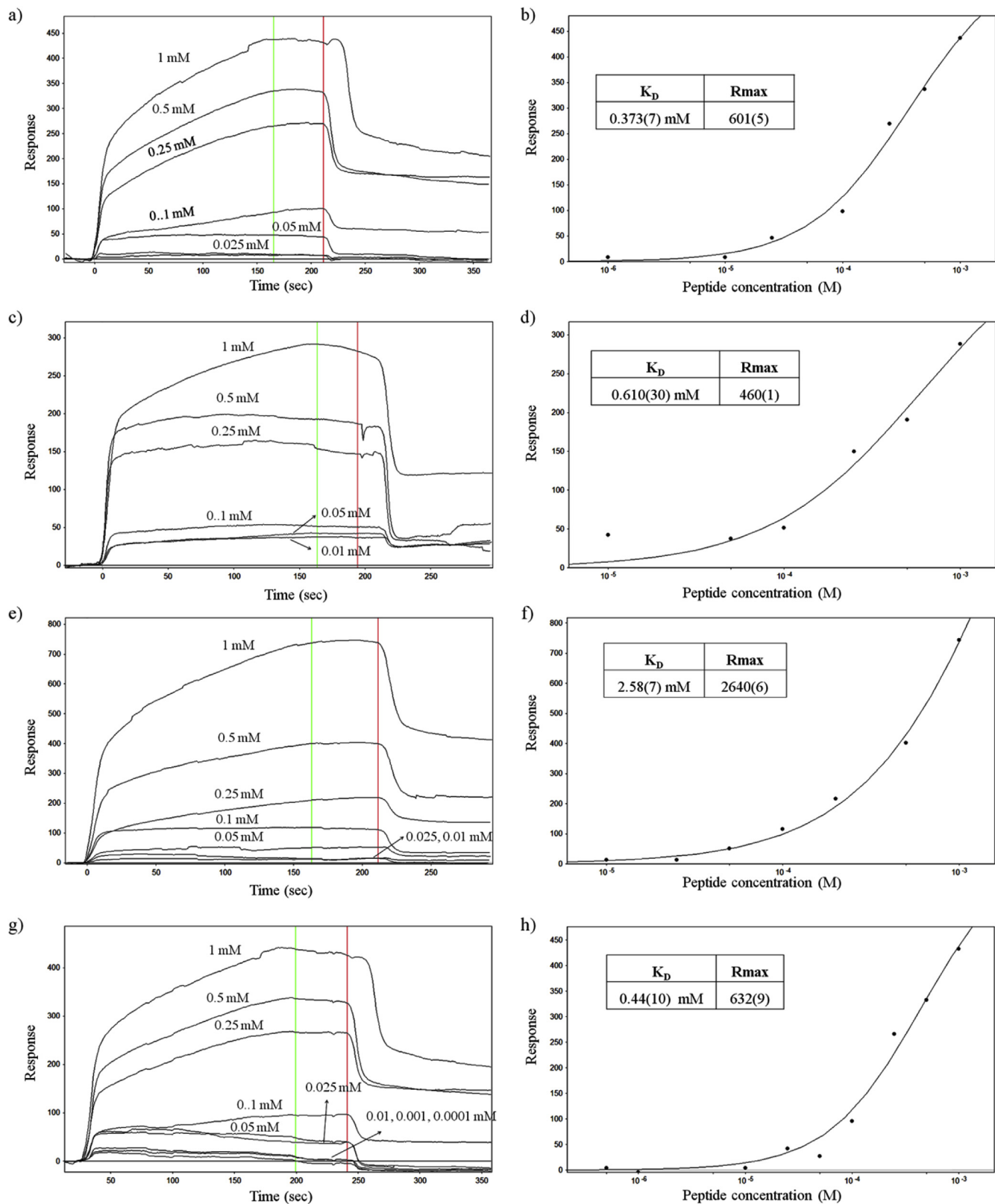


Fig. 12. Surface-plasmon resonance sensorgrams of the interaction of liposomes with peptide analogs. Dilution-series binding and dose-response plot of the interaction with POPC liposomes. a), b) Peptide **1**; c), d) Peptide **2**; e), f) Peptide **8** and g), h) Peptide **10**.

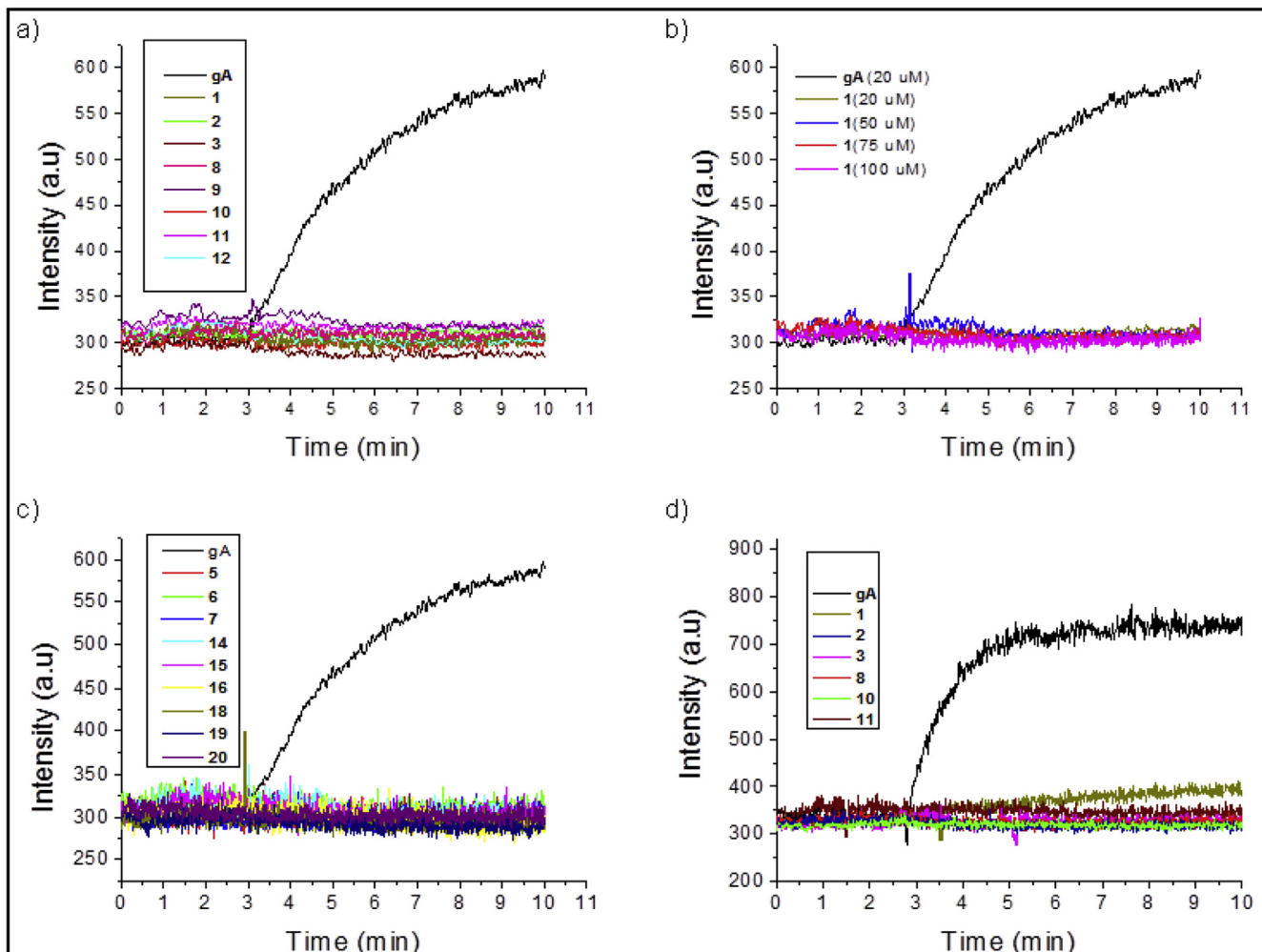


Fig. 13. Gramicidin A and its analogous peptide-caused lysis of a), b), c) POPC, and d) DOPC liposomes.

hexadecamer analogs at 20 μM concentration. Data reveals that **gA** causes 100% leakage with POPC liposomes; however, none of the analogs damaged POPC vesicles even at higher concentrations (**Fig. 13b**). No liposome leakage was observed with the shortened peptides as in **Fig. 13c**. The DOPC liposome leakage comparison of gramicidin A with hexadecamer analogs at 20 μM concentration of peptide analogs are plotted in **Fig. 13d**. **gA** causes 100% leakage with DOPC as well; however, none of the hexadecamer analogous peptides creates channels to liposome except peptide **1** where only 13% liposome leakage (**Fig. 13d**) was observed.

3.5. Antibacterial data analysis

The assessment of the antibacterial activity of azaproline-containing peptides and **gA** was performed using a standard minimal inhibitory concentration (MIC) test against *Escherichia coli*, *Klebsiella pneumoniae*, *Acinetobacter baumannii*, and *Staphylococcus aureus*. CO-ADD (The Community for Antimicrobial Drug Discovery), The University of Queensland (Australia) screened the antimicrobial activity. Colistin and vancomycin were used as positive inhibitor standards for gram-negative and gram-positive bacteria, respectively. All bacterial strain were cultured in cation-adjusted Muller Hinton broth (CAMHB) at 37 °C for 12 h. Cultured samples were diluted 40-fold in fresh broth and incubated at 37 °C for 1.5–3 h. The resultant mid-log phase cultures were diluted (CFU/

mL mesured by OD600), then 45 μL was added to each well of the compound-containing plates, giving a cell density of $5 \times 10^5 \text{ CFU/mL}$ and a final compound concentration of 32 $\mu\text{g}/\text{mL}$. Then all the plates were left standing at 37 °C for 18 h.

Growth inhibition was determined based on the amount of light scattered by the culture (by reading the optical density at 600 nm, OD600), using a Tecan M1000 Pro monochromator plate reader. Bacterial growth inhibition percentage was calculated for each well, using the negative control (media only) and positive control (bacteria without inhibitors) on the same plate as references. Z-score determine the significance of the inhibition values, which was calculated using the average and standard deviation of the sample wells (no controls) on the same plate. Samples with inhibition value above 80% and abs (Z-Score) above 2.5 were classed as actives and 20–80% as partial actives.

Initially, the compound **Gramicidin complex** (Cat BIA-G1592-1, bioaustralis fine chemicals) was subjected to whole cell growth inhibition assay as a 12-point dose response to determine the minimum inhibitory concentration (MIC) against. Two plate types were compared, non-binding surface (**NBS**) 96-well plates and polystyrene (**PS**) 96-well plates, assay was performed in duplicates ($n = 2$). The compound tested was found to be active only against *Staphylococcus aureus* (MRSA) with MIC 50–25 $\mu\text{g}/\text{mL}$ in polystyrene (**PS**) plates (**Table 2**). The compound was not active in the non-binding surface plates (**NBS**).

Table 2

Minimum inhibition concentrations (MIC) at 50 µg/mL of reference compounds (Vancomycin, Colistin and Gramicidin) against four bacterial pathogens.

Compound name	<i>E. coli</i>		<i>K. pneumoniae</i>		<i>A. baumannii</i>		<i>S. aureus</i>	
	FDA Control		MDR		Type		MRSA	
	NBS plate	PS plate	NBS plate	PS plate	NBS plate	PS plate	NBS plate	PS plate
Vancomycin	>32	>32	>32	>32	>32	>32	2	2
Vancomycin	>32	>32	>32	>32	>32	>32	2	2
Colistin	0.016	0.125	0.06	0.25	0.125	1	>32	>32
Colistin	0.016	0.125	0.06	0.25	0.06	1	>32	>32
Gramicidin	>50	>50	>50	>50	>50	>50	>50	50
Gramicidin	>50	>50	>50	>50	>50	>50	>50	25

Later we have isolated gramicidin A from the complex by HPLC 33–95% acetonitrile gradient over 30 min and characterized it by LCMS. The results, listed in Fig. 14, show activity for purified **gA** (17 µM) and its peptide analogs at 32 µg/mL which is 15–17 µM concentration depending on the molecular weight of hexadecamers. Data suggest that **gA** is much less active against *S. aureus* is 2.5 µM reported by Wang et al. [40,65]. Comparing the activity of Pro-AzPro peptides with earlier literature **gA** activity reveals that there is tremendous loss in activity of the analogs against *S. aureus*.

Data reveals that **gA** peptide analog **1** bearing Cbz group at *N*-terminus inhibits 38% of *A. baumannii* growth selectively, whereas **1**, **9**, **13** and **22** are selective with *S. aureus*. However, the full length 32mer (**11**) and peptides **2**, **4** and **14** display a considerable loss of activity. Hexadecameric peptides **16** and **17** as amine hydrochloride salts showed some activity with both *S. aureus* and *A. baumannii* and surprisingly, octamers **18**, **19**, **22** and **23** showed little inhibition.

Shortening the peptide length of Pro-AzPro oligomers (**5**, **6**, **14** and **20**) from hexadecamer in L&D-helical structure largely abolishes all activity with any of the five bacterial strains. The exact process of the membrane disruption is not completely understood [66]. This study demonstrates the presence of $\beta^{6,3}$ -helical structure alone in the **gA** analogs cannot be used for the prediction of potential antimicrobial activity and may indicate a more complicated mechanism.

3.6. Antifungal data analysis

Antifungal activity was measured by a quantitative microspectrophotometric assay. Fungi strains cultured for 3 days on Yeast Extract-Peptone Dextrose (YPD) agar at 30 °C. Cultured yeast suspension of 1–5 million cells/mL (as determined by OD530) was prepared from five colonies. These stock suspensions were diluted with Yeast Nitrogen Base (YNB) broth to a make final concentration of 2.5×10^3 CFU/mL. Then, 45 µL of the fungi suspension was added to each well of the compound-containing plates, giving a final

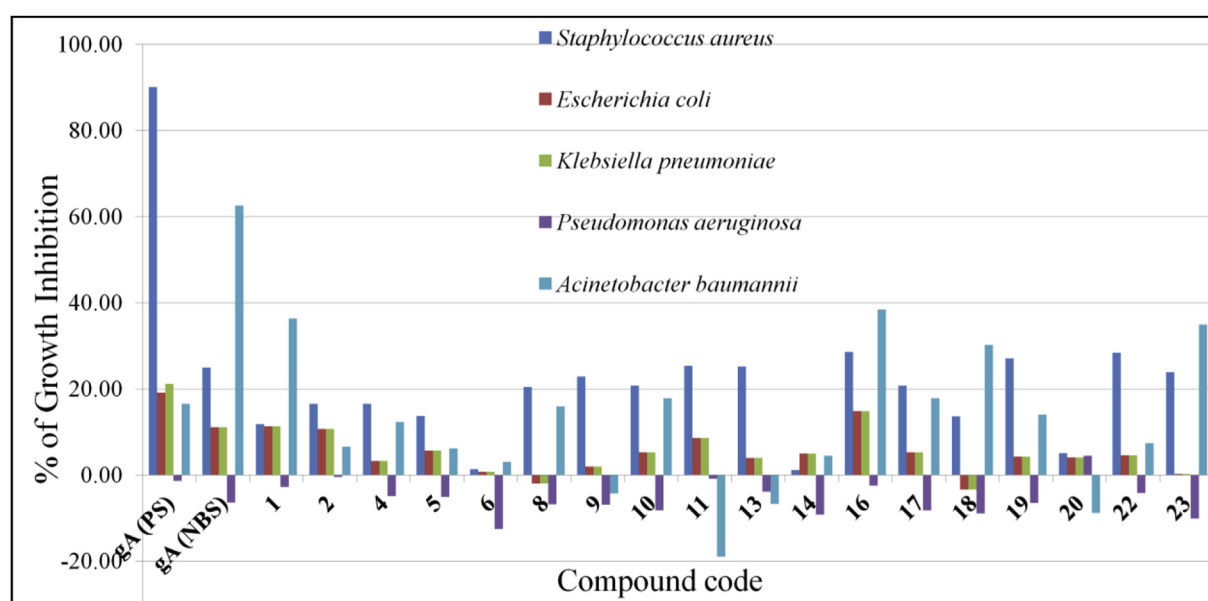


Fig. 14. Inhibition percentage of **gA** (17 µM) and its analogs against five bacterial pathogens.

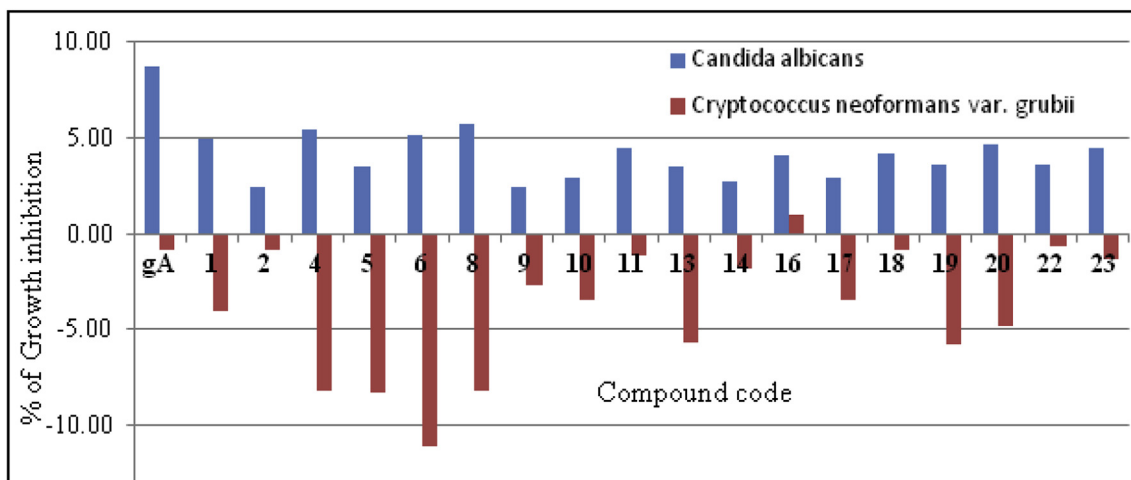


Fig. 15. Inhibition percentage (*C. albicans* = blue bars) of gramicidin A and its analogous peptides against two fungal pathogens. Note that growth of *C. neoformans* was enhanced (red bars). (For interpretation of the references to colour in this figure legend, the reader is referred to the Web version of this article.)

concentration of 32 µg/mL for the tested samples and incubated plates at 35 °C for 24 h without shaking. Fluconazole was used as a positive fungal inhibitor standard for *C. albicans* and *C. neoformans*.

Growth inhibition of *C. albicans* was determined based on the amount of light scattered by the culture at 530 nm (by reading the optical density at 530 nm, OD530 and *C. neoformans* growth inhibition was determined by measuring the difference in the amount of light scattered between 600 and 570 nm (OD600-570), after the addition of resazurin (0.001% final concentration) and incubation at 35 °C for an additional 2 h. Analysis of data reveals that the peptides inhibit the growth of *C. albicans* is found to be not more than 10% (Fig. 15) including **gA**. Surprisingly, these peptides enhance *C. neoformans* growth (Fig. 15).

3.7. Discussion and conclusion

In conclusion, the biomimetic syntheses of **gA** analogs including full length 32-residue channel peptide **11** was successfully demonstrated. Synthetic azaproline (AzPro) allowed generation of several **gA** analogs having L-Pro-AzPro and AzPro-L-Pro repeating units. The conservation of $\beta^{6,3}$ -helical character was confirmed for all 16-residue peptides, full length 32-residue peptide (**11**), and **gA** using circular dichroism. No ability to lyse liposomes was established suggesting a lack of channel formation, nor did these peptidomimetics hemolyze red blood cells, unlike gramicidin A. SPR binding assay study and liposome leakage experiment showed that analogous peptides just associated with lipid liposomes vesicles instead of rupturing them. Analysis of the antimicrobial activity of the 19 peptides revealed a lowered bactericidal effect for peptide analogs compared with **gA**. Apparently, modification of the **gA** with azaproline and proline residue is counterproductive with respect to antibacterial activity even when the $\beta^{6,3}$ -helical character is preserved. 16-mers having AzPro-Pro repeating unit (**1**, **8**, **13** and **9**) showed highest activity, surprisingly drastic loss in activity of the 32-mer (**11**), perhaps due to a length that was greater than the membranes width. No antifungal activity was observed for any of these analogs including **gA**. We hypothesize that introduction of lysine residues at the *N*-terminus region of the peptides should be explored in future development of **gA**-based peptidomimetic antibiotics.

3.8. Experimental section

1) Chemistry General:

All the reactions were performed in oven-dried apparatus and were stirred using magnetic stirbars. Starting materials, reagents, and solvents were purchased from commercial vendors unless otherwise noted. Chromatography grade ethylacetate, dichloromethane, acetonitrile, and hexanes were obtained from Sigma-Aldrich. Column chromatography was performed on silica gel (100–200 mess) purchased from Sorbent Technologies. TLC was carried out on Analtech 200 µm silica-gel coated plastic-fiber sheets. All reactions were monitored by thin layer chromatography (TLC) carried out on Merck silica-gel plates (0.25 mm thick, 60F254), visualized by using UV (254 nm) or dyes such as ninhydrin, KMnO₄, *p*-anisaldehyde or CAM (ceric ammonium molybdate). High-performance liquid chromatography (HPLC) was carried out on GILSON GX-281 using Waters C₁₈ 5 µM, 4.6 × 50 mm and Waters Prep C₁₈ 5 µM, 19 × 150 mm reverse phase columns. The mobile phases used were A: H₂O with 0.05% TFA, B: CH₃CN with 0.05% TFA using a solvent gradient of A-B over 30 min with a flow rate of 14.8 mL/min, with detection at 220 and 254 nm UV detectors. Purity assessment and mass spectra (MS) data were obtained using a Hewlett-Packard HPLC/MSD using electrospray ionization (ESI) for detection. ¹H and ¹³C NMR spectra were measured on a Varian 400 MHz NMR instrument. Chemical shifts are expressed in parts per million (ppm) from the residual of nondeuterated solvents as internal standard. (1H NMR: TMS = 0.00 ppm, CDCl₃ δ = 7.26 ppm, DMSO-d6 δ = 2.50 ppm, D₂O: δ = 4.79 ppm; ¹³C NMR (APT): TMS δ = 0.00 ppm, CDCl₃ δ = 77.16 ppm, DMSO-d6 δ = 39.52 ppm). Coupling constants (J) are given in hertz (Hz). The following abbreviations were used to express the multiplicities: s = singlet; d = doublet; t = triplet; q = quartet; p = pentet; quin = quintet; sep = septet; hept = heptet; m = multiplet; dd = doublet of doublets; dt = doublet of triplet; td = triplet of doublet; m = multiplet; bs = broad singlet. All compounds used for CD, liposome lysis SPR studies and biological assays were >95% pure based on NMR and LC-MS by UV absorbance at 210 nm and 254 nm wavelengths.

2) General Procedure for Azaproline Synthesis:

2a) Synthesis of Boc-NH-NH-Cbz (26): To a cold solution (0 °C) of *tert*-butyl hydrazinecarboxylate hydrochloride (7.1 g, 53.8 mmol) in and *N*-methylmorpholine (17.7 mL, 161 mmol) in tetrahydrofuran (100 mL) was added benzyl chloroformate (7.7 g, 53.8 mmol) and slowly brought to room temperature and stirred for 10 h.

Tetrahydrofuran was removed under reduced pressure and the resulting viscous solution was diluted with water (40 mL) and thoroughly extracted with ethyl acetate (50 × 3 mL). The combined organic extracts were washed with 1 N HCl (25 mL), saturated aqueous sodium bicarbonate (NaHCO_3) (25 mL) and dried over anhydrous sodium sulphate (Na_2SO_4) and concentrated to give a residue, which was purified by silica gel column chromatography (EtOAc:Hexane – 2:5) to give a white solid (13.8 g, yield: 96%). **$^1\text{H NMR}$ (400 MHz, CDCl_3) δ ppm:** 7.44–7.27 (m, 5 H), 6.48 (bs, 1 H), 6.29 (bs, 1 H), 5.18 (s, 1 H), 1.46 (bs, 9 H), MS (ESI): found: $[\text{M} + \text{Na}]^+$, 289.2.

2b) Boc-AzPro-Cbz (24): 55% Sodium hydride (2.1 g, 52.6 mmol) was taken into 250 mL round bottom flask under nitrogen atmosphere and dry hexane (25 mL) was added and stirred for 5 min, then removed hexane with syringe. Repeated this process twice to activate the sodium hydride from paraffin. Then Boc-NH-NH-Cbz (7 g, 26.3 mmol) in dry *N,N*-dimethylformamide (75 mL) was added to the activated sodium hydride and stirred at 0 °C for 10 min. Then 1,3-dibromopropane (2.65 mL, 26.3 mmol) was added dropwise over 10 min, slowly brought to room temperature and stirred for 3 h. Reaction was quenched with 1 N HCl and *N,N*-dimethylformamide was removed under reduced pressure and the resulting viscous solution was diluted with water (20 mL) and thoroughly extracted with ethyl acetate (40 × 3 mL), then dried over anhydrous sodium sulphate (Na_2SO_4) and concentrated to give a residue, which was purified by silica gel column chromatography (EtOAc:Hexane – 3:5) as a viscous oil (7.13 g, yield: 89%). **$^1\text{H NMR}$ (400 MHz, CDCl_3) δ ppm:** 7.42–7.27 (m, 5 H), 5.26 (d, $J = 11.9$ Hz, 1 H), 5.11 (d, $J = 11.8$ Hz, 1 H), 4.02–3.82 (m, 2 H), 3.34–3.26 (m, 1 H), 3.26–3.09 (m, 1 H), 2.04 (quin, $J = 7.1$ Hz, 2 H), 1.42 (s, 9 H). **$^{13}\text{C NMR}$ (100 MHz, CDCl_3) δ ppm:** 136.2, 128.4, 128.0, 127.9, 81.5, 77.3, 77.0, 76.7, 67.7, 46.7, 46.2, 28.1, 25.6. MS (ESI): found: $[\text{M} + \text{Na}]^+$, 329.3.

2c) TFA-AzPro-Cbz (28): Boc-AzPro-Cbz (5 g, 16.3 mmol) was dissolved in 15% trifluoroacetic acid in CH_2Cl_2 (50 mL) and stirred at 0 °C for 3 h. Solvent was removed by rotary evaporation, and the residue washed with hexane (3 × 10 mL) for removal of a trace amount of trifluoroacetic acid. The residue was dried *in vacuo* over a KOH trap to obtain the desired Boc deprotected amine salt as a viscous oil (5.56 g, yield: 100%) and used without further purification. MS (ESI): found: $[\text{M} + \text{Na}]^+$, 229.3.

2d) Cbz-AzPro-Pro-O^tBu (29): To a cold solution (–30 °C) of Boc-AzPro-H-TFA (4 g, 12.6 mmol) in dry tetrahydrofuran (THF) (50 mL) was added *N*-methylmorpholine (1.04 mL, 9.3 mmol) and triphosgene (1.3 g, 4.4 mmol) then stirred for 30 min. Then a solution of proline *t*-butyl ester hydrochloride (2.15 g, 12.6 mmol) in *N,N*-dimethylformamide (8 mL) was added to the flask followed by *N*-methylmorpholine (1.04 mL, 9.3 mmol) and the reaction mixture was slowly brought to room temperature and stirred till the starting material was consumed completely. *N,N*-dimethylformamide and tetrahydrofuran were removed under reduced pressure and the resulting viscous solution was diluted with water (10 mL) and thoroughly extracted with ethyl acetate (20 × 3 mL). The combined organic extracts were washed with 1 N HCl (15 mL), saturated aqueous sodium bicarbonate (NaHCO_3) (15 mL) and dried over anhydrous sodium sulphate (Na_2SO_4) and concentrated to give a residue, which was purified by silica gel column chromatography (EtOAc: Hexane – 2:3) as a viscous oil (4.1 g, yield: 82%). **$^1\text{H NMR}$ (400 MHz, CDCl_3) δ ppm:** 7.39–7.28 (m, 5 H), 5.22 (d, $J = 12.0$ Hz, 1 H), 5.15 (d, $J = 12.0$ Hz, 1 H), 4.48–4.40 (m, 1 H), 3.81–3.71 (m, 1 H), 3.71–3.60 (m, 2 H), 3.51 (td, $J = 6.4, 10.4$ Hz, 2 H), 3.41–3.23 (m, 1 H), 2.20–2.09 (m, 1 H), 2.04 (quin, $J = 7.2$ Hz, 2 H), 1.95–1.76 (m, 3 H), 1.44 (s, 9 H). MS (ESI): found: $[\text{M} + \text{Na}]^+$, 426.4.

3) HATU peptide coupling protocol for azaproline coupling:

To a solution (0 °C) of 1-[bis(dimethylamino)methylene]-1*H*-1,2,3-triazolo [4,5-*b*]pyridinium 3-oxid hexafluorophosphate (HATU) (1.3 mmol) in *N,N*-dimethylformamide (10 mL), *N,N*-diisopropylethylamine (3 mmol) was added and stirred for 15 min. Then added azaproline fragment (1 mmol) in *N,N*-dimethylformamide (4 mL) followed by DIEA (2 equivalents) and stirred it for 7–8 h at 4 °C, and the reaction mixture stirred at room temperature till the starting material was consumed completely. *N,N*-dimethylformamide was removed under reduced pressure and the resulting viscous solution was diluted with water (5 mL) and thoroughly extracted with ethyl acetate (15 mL). The combined organic extracts were washed with 1 N HCl (5 mL), saturated aqueous sodium bicarbonate (NaHCO_3) (5 mL) and dried over anhydrous sodium sulphate (Na_2SO_4) and concentrated to give a residue, which was purified by silica gel (100–200 mesh) flash column chromatograph.

4) General procedure for triphosgene coupling protocol:

To a cold solution (–30 °C) of Boc-AzPro-H (1.0 mmol) in dry tetrahydrofuran (THF) (5 mL) *N*-methylmorpholine (1.2 mmol) and triphosgene (0.35 mmol) were added and stirred for 30 min. Then a solution of amino acid ester hydrochloride (1 mmol) in *N,N*-dimethylformamide (2 mL) flask was added, followed by *N*-methylmorpholine (2.2 mmol) and the reaction mixture was slowly brought to room temperature and stirred till the starting material was consumed completely. *N,N*-dimethylformamide and dichloromethane were removed under reduced pressure and the resulting viscous solution was diluted with water (5 mL) and thoroughly extracted with ethyl acetate (15 mL). The combined organic extracts were washed with 1 N HCl (5 mL), saturated aqueous sodium bicarbonate (NaHCO_3) (5 mL) and dried over anhydrous sodium sulphate (Na_2SO_4) and concentrated to give a residue, which was purified by silica gel (100–200 mesh) flash column chromatograph.

5) General Procedure - Acidic cleavage of *N*-*tert*-butyloxycarbonyl (Boc) using trifluoroacetic acid:

The protected peptide (1.0 mmol) was dissolved in 15% trifluoroacetic acid in CH_2Cl_2 (5 mL) and stirred at 0 °C for 3 h. Solvent was removed by rotary evaporation and the residue washed with hexane (3 × 10 mL) for removal of a trace amount of trifluoroacetic acid. The residue was dried *in vacuo* over a KOH trap and used without further purification.

6) General Procedure - Acidic cleavage of O^tButylester (O^tBu) protecting group using trifluoroacetic acid:

The protected peptide (1.0 mmol) was dissolved in 30% trifluoroacetic acid in CH_2Cl_2 (5 mL) and stirred at 0 °C for 3 h. Solvent was removed by rotary evaporation and the residue washed with hexane and evaporated (3 × 10 mL) for removal of trace amounts of trifluoroacetic acid. The residue was dried *in vacuo* over a KOH trap and used without further purification.

Acknowledgements

The authors thank the Division of Biology and Biological Sciences at Washington University for a graduate fellowship (SS), the Washington University Career Center for an Undergraduate Summer Internship Award (SS), a gift from Suzanne and Garland Marshall to the Department of Chemistry to support undergraduate research, and the Department of Biochemistry and Molecular Biophysics, WUSM for research support. Antimicrobial screening was performed by CO-ADD (The Community for Antimicrobial Drug Discovery), funded by the Wellcome Trust (UK) and The University of

Queensland (Australia). We are grateful to Prof. Carl Frieden for providing access to his CD facility.

Appendix A. Supplementary data

Detailed experimental procedures, purity and spectral data of compounds, PDB coordinates in machine readable format for computational models, PDB reference IDs of gramicidin A, RBC hemolysis and antimicrobial activity data.

Predicted Models: The PDB coordinates of the predicted helical structure Ac-(Pro-AzPro)₁₄-COOMe (30 mer) and Ac-(Pro-AzPro)₈-Ac (16 mer-CaCl₂) complex in water.

Supplementary data related to this article can be found at <https://doi.org/10.1016/j.ejmech.2018.02.057>.

Abbreviation

AzPro	azaproline
MD	molecular dynamic
MMFF	Merck molecular force field
NVT	constant temperature, constant volume
RMSD	root-mean-square deviation
ADME	absorption, distribution, metabolism, and excretion
MIC	minimal inhibitory concentration
NMR	nuclear magnetic resonance spectroscopy
PDB	protein data bank
Cs	Caesium
SDS	Sodium dodecyl sulphate
DIEA	diisopropylethylamine
Boc	tert-butyloxycarbonyl
Cbz-Cl	carbobenzoxychloride
Cbz	carboxybenzyl
Fmoc-Cl	chloroformic acid 9H-fluoren-9-ylmethyl ester
DMAP	4-dimethylaminopyridine
NaH	Sodium hydride
DMF	N,N-dimethylformamide
O ^t Bu	ortho-tert-butyl
LiOH	lithium hydroxide
MeOH	methanol
EDC	1-ethyl-3-(3-dimethylaminopropyl)carbodiimide
HATU	1-[Bis(dimethylamino)methylene]-1H-1,2,3-triazolo[4,5-b]pyridinium 3-oxide hexafluorophosphate
DCM	dichloromethane
EtOAc	ethylacetate
DMSO	dimethyl sulfoxide
PBS	phosphate-buffered saline
BSA	bovine serum albumin
POPC	1-palmitoyl-2-oleoyl-sn-glycero-3-phosphocholine
DOPC	1,2-dioleoyl-sn-glycero-3-phosphocholine
KCl	Potassium chloride
HCl	hydrochloric acid
TFA	trifluoroacetic acid
HPLC	high performance liquid chromatography
SPR	surface plasmon resonance

References

- [1] E. Cabezas, A.C. Satterthwait, The hydrogen bond mimic approach: solid-phase synthesis of a peptide stabilized as an α -helix with a hydrazone link, *J. Am. Chem. Soc.* 121 (1999) 3862–3875.
- [2] R.N. Chapman, G. Dimartino, P.S. Arora, A highly stable short α -helix constrained by a main-chain hydrogen-bond surrogate, *J. Am. Chem. Soc.* 126 (2004) 12252–12253.
- [3] H.E. Stanger, S.H. Gellman, Rules for antiparallel β -sheet design: D-Pro-Gly is superior to L-Asn-Gly for β -hairpin Nucleation, *J. Am. Chem. Soc.* 120 (1998) 4236–4237.
- [4] J.P. Schneider, J.W. Kelly, Templates that induce α -helical, β -sheet, and loop conformations, *Chem. Rev.* 95 (1995) 2169–2187.
- [5] D.S. Kemp, B.R. Bowen, C.C. Muendel, Synthesis and conformational analysis of epindolidione-derived peptide models for β -sheet formation, *J. Org. Chem.* 55 (1990) 4650–4657.
- [6] J.D. Fisk, S.H. Gellman, A parallel β -sheet model system that folds in water, *J. Am. Chem. Soc.* 123 (2000) 343–344.
- [7] D.N. Reddy, R. Thirupathi, E.N. Prabhakaran, Accessing the disallowed conformations of peptides employing amide-to-imidate modification, *Chem. Commun.* 47 (2011) 9417–9419.
- [8] S. Tumminakatti, D.N. Reddy, E.N. Prabhakaran, Exploring the consequences of a representative “disallowed” conformation of Aib on a 3₁₀-helical fold, *Bio-polymers* 104 (2015) 21–36.
- [9] R.R. Ketcham, K.-C. Lee, S. Huo, T.A. Cross, Macromolecular structural elucidation with solid-state NMR-derived orientational constraints, *J. Biomol. NMR* 8 (1996) 1–14.
- [10] G.N. Ramachandran, R. Chandrasekaran, Studies on dipeptide conformation and on peptides with sequences of alternating L and D residues with special reference to antibiotic and ion transport peptides, *Prog. Peptides Res.* 2 (1972) 195–215.
- [11] G.N. Ramachandran, R. Chandrasekaran, Conformation of peptide chains containing both L- & D-residues: Part I - helical structures with alternating L- & D-residues with special reference to the LD-ribbon & the LD-helix, *Indian J. Biochem. Biophys.* 9 (1972) 1–11.
- [12] V.F. Bystrov, A.S. Arseniev, Diversity of the gramicidin A spatial structure: two-dimensional ¹H NMR study in solution, *Tetrahedron* 44 (1988) 925–940.
- [13] Y. Chen, A. Tucker, B.A. Wallace, Solution structure of a parallel left-handed double-helical gramicidin-A determined by 2D ¹H NMR, *J. Mol. Biol.* 264 (1996) 757–769.
- [14] D.A. Doyle, B.A. Wallace, Shifting the equilibrium mixture of gramicidin double helices toward a single conformation with multivalent cationic salts, *Biophys. J.* 75 (1998) 635–640.
- [15] A. Olczak, M.L. Glowka, M. Szczesio, J. Bojarska, Z. Wawrzak, W.L. Duax, The first crystal structure of a gramicidin complex with sodium: high-resolution study of a nonstoichiometric gramicidin D-Nal complex, *Acta Crystallogr. D Biol. Crystallogr.* 66 (2010) 874–880.
- [16] R.J. Dubos, Studies on a bactericidal agent extracted from a soil bacillus : ii. Protective effect of the bactericidal agent against experimental pneumococcus infections in mice, *J. Exp. Med.* 70 (1939) 11–17.
- [17] R.J. Dubos, Studies on a bactericidal agent extracted from a soil *Bacillus* : i. Preparation of the agent. Its activity *in vitro*, *J. Exp. Med.* 70 (1939) 1–10.
- [18] R.J. Dubos, C. Cattaneo, Studies on a bactericidal agent extracted from a soil *bacillus* : iii. preparation and activity of a protein-free fraction, *J. Exp. Med.* 70 (1939) 249–256.
- [19] B.G. Dzikovski, P.P. Borbat, J.H. Freed, Channel and nonchannel forms of spin-labeled gramicidin in membranes and their equilibria, *J. Phys. Chem. B* 115 (2011) 176–185.
- [20] R. Sarges, B. Witkop, Gramicidin. VII. The structure of valine- and isoleucine-gramicidin B, *J. Am. Chem. Soc.* 87 (1965) 2027–2030.
- [21] R. Sarges, B. Witkop, A. Gramicidin Vi, The synthesis of valine- and isoleucine-gramicidin A, *J. Am. Chem. Soc.* 87 (1965) 2020–2027.
- [22] R. Sarges, B. Witkop, A.V. Gramicidin, The structure of valine- and isoleucine-gramicidin A, *J. Am. Chem. Soc.* 87 (1965) 2011–2020.
- [23] D.W. Urry, M.C. Goodall, J.D. Glickson, D.F. Mayers, The gramicidin A trans-membrane channel: characteristics of head-to-head dimerized (L,D) helices, *Proc. Natl. Acad. Sci. U.S.A.* 68 (1971) 1907–1911.
- [24] T.A. Cross, A. Arseniev, B.A. Cornell, J.H. Davis, J.A. Killian, R.E. Koeppe, L.K. Nicholson, F. Separovic, B.A. Wallace, Gramicidin channel controversy—revisited, *Nat. Struct. Biol.* 6 (1999) 610–611 discussion 611–612.
- [25] F. Kovacs, J. Quine, T.A. Cross, Validation of the single-stranded channel conformation of gramicidin A by solid-state NMR, *Proc. Natl. Acad. Sci. U.S.A.* 96 (1999) 7910–7915.
- [26] R.R. Ketcham, K.C. Lee, S. Huo, T.A. Cross, Macromolecular structural elucidation with solid-state NMR-derived orientational constraints, *J. Biomol. NMR* 8 (1996) 1–14.
- [27] B.M. Burkhardt, N. Li, D.A. Langs, W.A. Pangborn, W.L. Duax, The conducting form of gramicidin A is a right-handed double-stranded double helix, *Proc. Natl. Acad. Sci. U.S.A.* 95 (1998) 12950–12955.
- [28] A.L. Lomize, V. Orekhov, A.S. Arsen'ev, Refinement of the spatial structure of the gramicidin A ion channel, *Bioorg. Khim.* 18 (1992) 182–200.
- [29] B.M. Burkhardt, R.M. Gassman, D.A. Langs, W.A. Pangborn, W.L. Duax, Heterodimer formation and crystal nucleation of gramicidin D, *Biophys. J.* 75 (1998) 2135–2146.
- [30] A. Chaudhuri, S. Halder, H. Sun, R.E. Koeppe 2nd, A. Chattopadhyay, Importance of indole N-H hydrogen bonding in the organization and dynamics of gramicidin channels, *Biochim. Biophys. Acta* 1838 (2014) 419–428.
- [31] H. Gu, K. Lum, J.H. Kim, D.V. Greathouse, O.S. Andersen, R.E. Koeppe, The membrane interface dictates different anchor roles for “inner pair” and “outer pair” tryptophan indole rings in gramicidin A channels, *Biochemistry* 50 (2011) 4855–4866.
- [32] S. Halder, A. Chaudhuri, H. Gu, R.E. Koeppe, M. Kombrabail, G. Krishnamoorthy, A. Chattopadhyay, Membrane organization and dynamics of “inner pair” and “outer pair” tryptophan residues in gramicidin channels, *J. Phys. Chem. B* 116 (2012) 11056–11064.
- [33] D.W. Urry, S. Alonso-Romanowski, C.M. Venkatachalam, T.L. Trapane, K.U. Prasad, The source of the dispersity of gramicidin A single-channel

- conductances. The L X Leu5-gramicidin A analog, *Biophys. J.* 46 (1984) 259–265.
- [34] T.L. Jones, R. Fu, F. Nielson, T.A. Cross, D.D. Busath, Gramicidin channels are internally gated, *Biophys. J.* 98 (2010) 1486–1493.
- [35] Y. Mo, T.A. Cross, W. Nerdal, Structural restraints and heterogeneous orientation of the gramicidin A channel closed state in lipid bilayers, *Biophys. J.* 86 (2004) 2837–2845.
- [36] J. Yoo, Q. Cui, Membrane-mediated protein-protein interactions and connection to elastic models: a coarse-grained simulation analysis of gramicidin A association, *Biophys. J.* 104 (2013) 128–138.
- [37] I. Basu, A. Chattopadhyay, C. Mukhopadhyay, Ion channel stability of Gramicidin A in lipid bilayers: effect of hydrophobic mismatch, *Biochim. Biophys. Acta* 1838 (2014) 328–338.
- [38] J.A. Lundbaek, S.A. Collingwood, H.I. Ingolfsson, R. Kapoor, O.S. Andersen, Lipid bilayer regulation of membrane protein function: gramicidin channels as molecular force probes, *Journal of the Royal Society, Interface/the Royal Society* 7 (2010) 373–395.
- [39] J.W. Liou, Y.J. Hung, C.H. Yang, Y.C. Chen, The antimicrobial activity of gramicidin A is associated with hydroxyl radical formation, *PLoS One* 10 (2015), e0117065.
- [40] F. Wang, L. Qin, C.J. Pace, P. Wong, R. Malonis, J. Gao, Solubilized gramicidin A as potential systemic antibiotics, *ChemBioChem* 13 (2012) 51–55.
- [41] J. Mao, T. Kuranaga, H. Hamamoto, K. Sekimizu, M. Inoue, Rational design, synthesis, and biological evaluation of lactam-bridged gramicidin A analogues: discovery of a low-hemolytic antibacterial peptide, *ChemMedChem* 10 (2015) 540–545.
- [42] A.I. Sorochkina, E.Y. Plotnikov, T.I. Rokitskaya, S.I. Kovalchuk, E.A. Kotova, S.V. Sychev, D.B. Zorov, Y.N. Antonenko, N-terminally glutamate-substituted analogue of gramicidin A as protonophore and selective mitochondrial uncoupler, *PLoS One* 7 (2012), e41919.
- [43] D.N. Silachev, L.S. Khailova, V.A. Babenko, M.V. Gulyaev, S.I. Kovalchuk, L.D. Zorova, E.Y. Plotnikov, Y.N. Antonenko, D.B. Zorov, Neuroprotective effect of glutamate-substituted analog of gramicidin A is mediated by the uncoupling of mitochondria, *Biochim. Biophys. Acta* 1840 (2014) 3434–3442.
- [44] G.W. Gokel, S. Negin, Synthetic ion channels: from pores to biological applications, *Acc. Chem. Res.* 46 (2013) 2824–2833.
- [45] P. Xin, P. Zhu, P. Su, J.L. Hou, Z.T. Li, Hydrogen-bonded helical hydrazide oligomers and polymer that mimic the ion transport of gramicidin A, *J. Am. Chem. Soc.* 136 (2014) 13078–13081.
- [46] M. Barboiu, Y. Le Duc, A. Gilles, P.A. Cazade, M. Michau, Y. Marie Legrand, A. van der Lee, B. Coasne, P. Parvizi, J. Post, T. Fyles, An artificial primitive mimic of the gramicidin A channel, *Nat. Commun.* 5 (2014) 4142.
- [47] Y. Takeuchi, G.R. Marshall, Conformational analysis of reverse-turn constraints by *N*-methylation and *N*-hydroxylation of amide bonds in peptides and non-peptide mimetics, *J. Am. Chem. Soc.* 120 (1998) 5363–5372.
- [48] D.K. Chalmers, G.R. Marshall, Pro-D-NMe-amino acid and D-Pro-NMe-amino acid – simple, efficient reverse-turn constraints (Vol. 117, Pg 5927, 1995) (Additions & Corrections), *J. Am. Chem. Soc.* 118 (1996) 1579.
- [49] L.E. Townsley, The Three-dimensional Structure of Gramicidin Analogs in Micellar Environments Determined Using Two-dimensional Nuclear Magnetic Resonance Spectroscopic Techniques, Ph.D. Dissertation, University of Arkansas, Fayetteville, AR, USA, 2000.
- [50] W.J. Zhang, A. Berglund, J.L. Kao, J.P. Couty, M.C. Gershengorn, G.R. Marshall, Impact of azaproline on amide *cis-trans* isomerism: conformational analyses and NMR studies of model peptides including TRH analogues, *J. Am. Chem. Soc.* 125 (2003) 1221–1235.
- [51] Y. Zhang, R.M. Malamakal, D.M. Chenoweth, A single stereodynamic center modulates the rate of self-assembly in a biomolecular system, *Angew. Chem. Int. Ed. Engl.* 54 (2015) 10826–10832.
- [52] M.I. Calaza, C. Cativiela, Stereoselective synthesis of quaternary proline analogues, *Eur. J. Org. Chem.* 2008 (2008) 3427–3448.
- [53] Y. Che, G.R. Marshall, Impact of azaproline on peptide conformation, *J. Org. Chem.* 69 (2004) 9030–9042.
- [54] Y. Che, G.R. Marshall, Impact of *cis-proline* analogs on peptide conformation, *Biopolymers* 81 (2006) 392–406.
- [55] T.A. Halgren, Merck molecular force field. I. Basis, form, scope, parameterization, and performance of MMFF94, *J. Comput. Chem.* 17 (1996) 490–519.
- [56] W.L. DeLano, The PyMOL Molecular Graphics System, Version 1.6, 2002. Schrödinger, LLC.
- [57] F. Andre, M. Marraud, T. Tsouloufis, S.J. Tzartos, G. Boussard, Triphosgene: an efficient carbonylating agent for liquid and solid-phase aza-peptide synthesis. Application to the synthesis of two aza-analogues of the AChR MIR decapetide, *J. Pept. Sci.* 3 (1997) 429–441.
- [58] W.R. Veatch, E.T. Fossel, E.R. Blout, Conformation of gramicidin A, *Biochemistry* 13 (1974) 5249–5256.
- [59] Y. Chen, B.A. Wallace, Solvent effects on the conformation and far UV CD spectra of gramicidin, *Biopolymers* 42 (1997) 771–781.
- [60] D.W. Urry, D.F. Mayers, J. Haider, Spectroscopic studies on the conformation of gramicidin A'. Evidence for a new helical conformation, *Biochemistry* 11 (1972) 487–493.
- [61] M. Bouchard, D.R. Benjamin, P. Tito, C.V. Robinson, C.M. Dobson, Solvent effects on the conformation of the transmembrane peptide gramicidin A: insights from electrospray ionization mass spectrometry, *Biophys. J.* 78 (2000) 1010–1017.
- [62] J.A. Killian, Gramicidin and gramicidin-lipid interactions, *Biochim. Biophys. Acta* 1113 (1992) 391–425.
- [63] F. Wang, L. Qin, C.J. Pace, P. Wong, R. Malonis, J. Gao, Solubilized gramicidin A as potential systemic antibiotics, *ChemBioChem* 13 (2012) 51–55.
- [64] M. Saito, S.J. Korsmeyer, P.H. Schlesinger, BAX-dependent transport of cytochrome c reconstituted in pure liposomes, *Nat. Cell Biol.* 2 (2000) 553–555.
- [65] F. Wang, L. Qin, P. Wong, J. Gao, Effects of lysine methylation on gramicidin A channel folding in lipid membranes, *Biopolymers* 100 (2013) 656–661.
- [66] E.J. Prenter, R.N.A.H. Lewis, R.N. McElhaney, The interaction of the antimicrobial peptide gramicidin S with lipid bilayer model and biological membranes, *Biochim. Biophys. Acta Biomembr.* 1462 (1999) 201–221.